The Hot Atom Production Loop

The investigation of a new radionuclide production loop based on the Szilard-Chalmers effect

M.M. Naaktgeboren

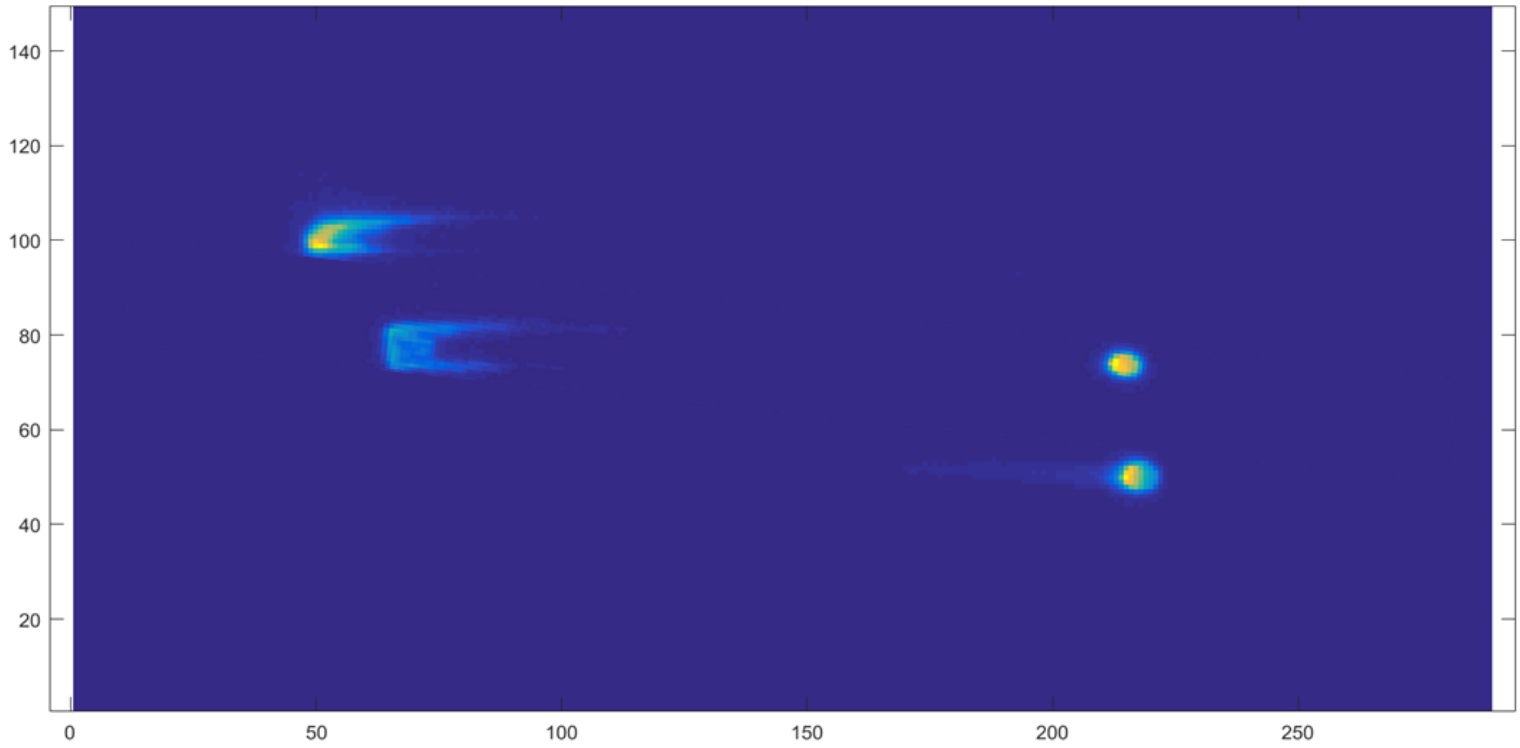

TU Delft

The Hot Atom Production Loop

The investigation of a new radionuclide production loop based on the Szilard-Chalmers effect

by

M.M. Naaktgeboren

this thesis is part of the Master Applied Physics
at the Delft University of Technology,
to be defended publicly on Thursday May 27, 2021 at 10:00 AM.

Student number:	4569644	
Project duration:	October 1, 2020 – May 27, 2021	
Supervisor:	Dr. ir. R.M. de Kruijff,	TU Delft
Thesis committee:	Dr. ir. A.G. Denkova,	TU Delft
	Dr. ir. M. Rohde,	TU Delft

An electronic version of this thesis is available at `http://repository.tudelft.nl/`.

TU Delft

Abstract

Radionuclides are important in the diagnosis and treatment of, amongst others, cancer. A promising therapy is targeted radionuclide therapy, where the radionuclide is brought to the tumor by a targeting specific vector. Bringing the radionuclide directly to the tumor, should reduce the dose to the healthy tissue. For targeted radionuclide therapy, a radionuclide with a high specific activity is required. Some radionuclides, with promising half-lives and decay energies, are currently not produced with the required specific activity. This problem occurs mainly for radionuclides that are produced via (n,γ) reactions in nuclear reactors. For radionuclides that are produced via this reaction, it is nearly impossible to do a chemical separation between the target material and the produced radionuclide, because these are of the same element. This is why new production routes have to be investigated.

In this thesis a feasibility study has been done for a new production method, which should increase the specific activity of radionuclides that are produced via a (n,γ) reaction. For this production method, the target material is labeled with a chelator. Due to the Szilard-Chalmers effect the bond with the chelator will be broken, when the target material is activated by a neutron. This enables the separation of the produced radionuclide from the target complex and therefore, the extraction of the radionuclide. The production method will be loop-based, in order to enable continuous activation of the target material and extraction of the radionuclide. Furthermore, the loop-based design should minimize the effect of radiolysis and relabeling. The loop will be placed close to the reactor core. In this thesis, the elements holmium and lutetium have been used. It has been determined which chelator is most suitable to label with holmium and lutetium. Furthermore, the stability of this complex has been investigated for: higher temperatures, time and the effect of the γ-radiation. The effect of the γ-radiation was determined because this results in radiolysis. The extraction of the radionuclide has also been investigated. These parameters have been used in the calculation of the possible achievable specific activity of ^{166}Ho and ^{177}Lu, when using this loop-based production method.

Labeling was possible with the chelator DOTA, which resulted in a stable complex, even for higher temperatures. Labeling happened fast, which also results in fast relabeling. The effect of radiolysis, due to the γ-radiation, was determined by fitting the experimental data. The fit gave negative values for short irradiation times, which is not possible. Therefore, two possible fits were made, which did not give negative results. The first fit was shifted over the y-axis and for the second fit the negative values were assigned to be zero. Because the fit of the data points had to be adapted, this shows that there is a large uncertainty of the radiolysis at short irradiation times. Extraction of free lutetium from LuDOTA is possible using Dowex resins.

When taking into account the experimentally determined factors, as well as the recoiling factor from the literature, the following results for the achievable specific activities of holmium and lutetium were obtained. For holmium, the specific activity without the Szilard-Chalmers effect and the loop is $SA_{withoutSZ}$ = 0.93 GBq/mg. When using the shifted function for the radiolysis, $fs_{radiolysis}$, the calculated specific activities are $SA_{withSZloop}$ = 3.21 GBq/mg with the loop and SA_{withSZ} = 6.40 GBq/mg with only the Szilard-Chalmers effect. When the cut-off radiolysis function, $fc_{radiolysis}$, is used, the calculated specific activities are $SA_{withSZloop}$ = 22015 GBq/mg with the loop and SA_{withSZ} = 6.79 GBq/mg with only the Szilard-Chalmers effect. For lutetium the specific activity without the loop and SZ effect is $SA_{withoutSZ}$ = 0.76 GBq/mg. When using the shifted function for the radiolysis, the calculated specific activities are $SA_{withSZloop}$ = 1.31 GBq/mg with the loop and SA_{withSZ} = 2.39 GBq/mg with only the Szilard-Chalmers effect. When the cut-off radiolysis function is used, the calculated specific activities are $SA_{withSZloop}$ = 89.9 GBq/mg with the loop and SA_{withSZ} = 2.76 GBq/mg with only the Szilard-Chalmers effect. This concludes that using the Szilard-Chalmers effect in the production of radionuclides increases the specific activity. It might be possible to have an even higher specific activity, when using the loop-based production, however, this is very dependant on the radiolysis for short irradiation times, which had a high uncertainty in the calculations. To be able to determine if the loop system is beneficial, the radiolysis for short irradiation times has to be determined.

Contents

List of Abbreviations

BPAMD	4-[bis-(phosphonomethyl))carbamoyl]methyl-7,10-bis(carboxy methyl) -1,4,7,10-tetraazacyclododec-1-yl)acetic acid
cyclam	1,4,8,11-Tetra-azacyclotetradecaan
DTPA	Diethylenetriaminepentaacetic acid
DOTA	1,4,7,10-Tetraazacyclododecane-1,4,7,10-tetraaceticacid
EDTA	Ethylenedinitrilotetraacetic acid
FlexBeFa	Flexibele Bestralings Faciliteit (Flexible irradiation facility)
HCl	Hydrochloric Acid
Ho	Holmium with a natural abundance of 100% ^{165}Ho
HoDOTA	Labeled Ho with DOTA
HoDTPA	Labeled Ho with DTPA
HoEDTA	Labeled Ho with EDTA
HOR	Hoger Onderwijs Reactor (Higher Education Reactor)
iTLC	Instant Thin Layer Chromatography
Lu	Lutetium with the natural occurring abundance
LuDOTA	Lu labeled with DOTA
LuDTPA	Lu labeled with DTPA
LuEDTA	Lu labeled with EDTA
MQ	MilliQ water
NH_4Ac	Ammonium acetate
NTA	Nitrilotriacetic acid
NMR	Nuclear magnetic resonance
PET	Positron emission tomography
rpm	Rounds per minute
RT	Room temperature
SA	Specific activity
Sf	Solvent front
SPECT	Single photon emission computed tomography
SZ effect	Szilard-Chalmers effect
TRT	Targeted radionuclide therapy

1

Introduction

Radioisotopes have several applications, such as in nuclear medicine and the oil and gas industry [1]. The demand for radioisotopes is the highest in nuclear medicine, since worldwide every year around 30-50 million patients are diagnosed using radionuclides or treated with radionuclides, in over 10,000 hospitals [2]. A promising group of radionuclides are the radiolanthanides, the lanthanides are a group of elements with their atomic number from 57-71 [3]. Since the lanthanides have very similar chemical properties [4], this could lead to a group of radionuclides with different half-lives and decay energies, from which can be chosen depending on the treatment [5]. Many radiolanthanides are produced in nuclear reactors, via a (n,γ) reaction [6]. When the production is done via a (n,γ) reaction, the target material and the produced radionuclide are of the same element. In this thesis, the target material is defined as the stable nuclide that is labeled with a chelator and irradiated. The produced radionuclide is the product of the (n,γ) reaction of the target material. Since the target material and the produced radionuclide are of the same element, it is nearly impossible to have a separation between the irradiated target and the produced radionuclide, since they are chemically identical [7]. This results in a low specific activity (SA), the activity divided by the sum of the mass of all the isotopes of the element in question that are present in the solution. The low specific activity is a problem for certain treatments [8]. Therefore, alternative production routes are investigated which could lead to a higher specific activity [9].

In this thesis, a method is investigated to increase the specific activity of radionuclides, that are produced via a (n,γ) reaction. The target material, a lanthanide, will be labeled with a chelator. Once the target material is excited by a neutron, the bond between the excited nuclide and the chelator will be broken, due to the Szilard-Chalmers effect [10]. As a result of this, it is possible to separate the produced radionuclide from the target material, because the target material is still coupled to a chelator and hence, chemically different from the produced radionuclide. This separation will happen during the irradiation, in order to reduce relabeling of the radionuclide with the chelator. Furthermore, the γ-radiation, that comes from the reactor core, affects the stability of the lanthanide-chelator complex. This can result in radiolysis [11], a ruptured bond between the target material and the chelator. This will lower the specific activity, because the target material is chemically the same and cannot be separated from the produced radionuclide. because of this, the radiolysis has to be minimized. In order to have continuous activation, continuous extraction and minimization of the effect of radiolysis, the production method will be loop-based. This loop will be placed close to the reactor core.

The use of the Szilard-Chalmers effect, for the production of high specific activity radionuclides that are produced via a (n,γ) reaction, shows to be promising, based on some research that has already been done. This research has been done for: ^{99}Mo [12, 13], ^{166}Ho [14–16], ^{186}Re and ^{188}Re [17].

The aim of this thesis is to investigate the feasibility of achieving a higher specific activity, for radionuclides that are produced via (n,γ) reactions. In this thesis the elements holmium (Ho) and lutetium (Lu) are used. Holmium was selected, because some promising research has already been done on producing holmium with a higher specific activity, when using the Szilard-Chalmers effect [14–16] . Lutetium was chosen, because it has a high cross section, which enhances the chance of excitation via a (n,γ) reaction. The investigation of the feasibility of a loop-based production, for higher specific activity radionuclides, will be done by looking at different requirements for the loop. The requirements include: to be able to label the

target material with a chelator, to determine the stability of this lanthanide-chelator complex and to determine how the extraction of the produced radionuclide can be done. These requirements have an effect on the achievable specific activity when using this loop-based production. Once it is known if labeling and extraction are possible and how stable the complex is, this can be used to determine the possible achievable specific activity for the produced radionuclide in the loop. These different requirements of the production loop are investigated by answering the following research questions:

1. Which lanthanide-chelator complexes can be used in the loop-based production?
2. What are the effects of temperature and gamma radiation on the stability of various lanthanide-chelator complexes?
3. Which extraction method can be used for instant separation of the produced radionuclide from the target material?
4. When taking into account the aspects above, what is the possible achievable specific activity when using this loop-based production?

In Chapter 2 the theoretical background on which this thesis is based is given. The used methods and materials for the experiments are described in Chapter 3, as well as the reasoning behind the programming script to determine the achievable specific activity. The results of the experiments and the calculations are given and discussed in Chapter 4. In Chapter 5 the conclusion is given by answering the research questions. Also recommendations for further research are given in this chapter. In Appendix A some additional figures are given of the fitted radiolysis functions and the calculated specific activities and in Appendix B the Python code for the specific activity calculations is given.

2

Theoretical Background

In this chapter the relevant theoretical background for this thesis is given. While the focus is on two elements, holmium and lutetium, the concepts in this chapter can also be applied to other elements.

2.1. Radionuclides in medical applications

There are two main applications for radionuclides in medical applications, namely imaging and treatment [18]. Single photon emission computed tomography (SPECT) is one of the main imaging techniques, using γ-ray emitting radionuclides such as ^{99m}Tc [19]. Another imaging technique is positron emission tomography (PET), using positron emitters such as ^{18}F [20]. The imaging techniques can for example be used for diagnosis of malignancies [21]. Some other examples of the use of radionuclides in medical applications are given in Figure 2.1. These radionuclides emit α-, β-particles or auger electrons that damage the DNA of the tumor which can result in apoptosis [22].

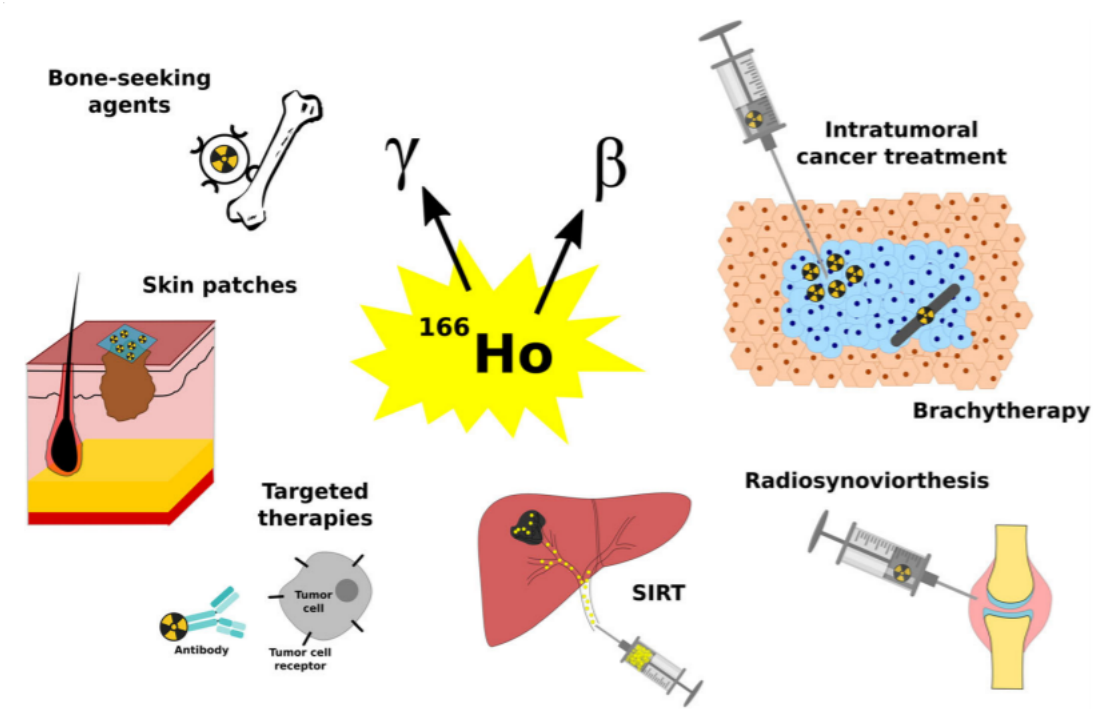

Figure 2.1: Different medical applications for the radionuclide ^{166}Ho, with the γ and β indicating emissions. The β-emission is used for treatment and γ-emission can be used for real-time imaging [23].

An important aspect of cancer treatment is to reduce the damage to the healthy tissue. An option to effectively target the tumor cell is targeted radionuclide therapy (TRT) [24]. In TRT the radionuclide is bound to a targeting vector, which interacts with the tumor [25]. In Figure 2.2 a schematic representation of TRT is given. The β-radiation of ^{177}Lu is used for the treatment, ^{177}Lu also emits γ-radiation which can be used for real-time imaging during the treatment [26]. A limiting factor in TRT is the amount of available target receptors on the tumor [27]. Therefore it is favorable to have 100% isotopic abundance of the needed radionuclide injected, i.e. then every target receptor is optimally used for the treatment. The specific activity is the activity divided by the sum of the masses of all isotopes of the element in question present in the injection [28]. Meaning, if there is less contamination of other isotopes in the solution, this results in a higher specific activity. This makes the achievable specific activity one of the characteristics on which the radionuclide is chosen for TRT. Some of the other factors are: the physical half-life, decay products, decay energy and potential of fast attachment to the targeting vector [25].

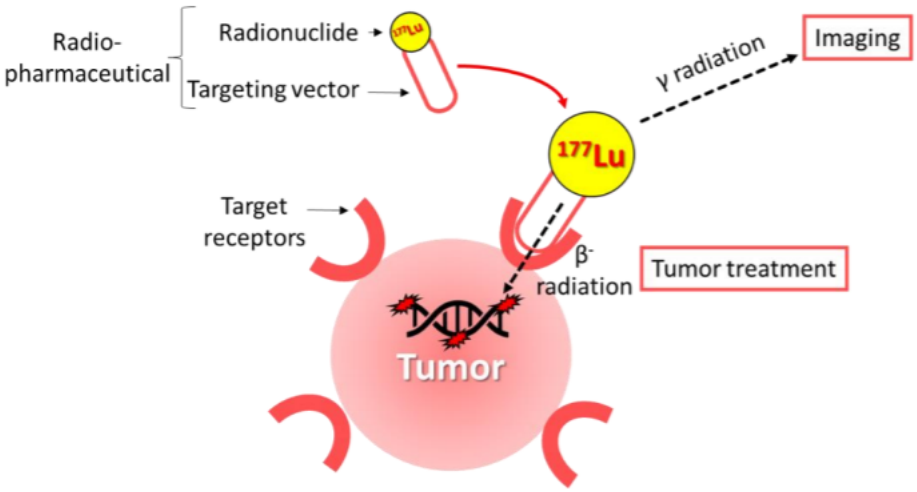

Figure 2.2: A schematic overview of targeted radionuclide therapy [25].

2.2. Decay schemes

The decay energy and decay products of a certain isotope can be obtained from the decay scheme, often also the half-life is given. For each decay route the yield is given. The decay schemes of ^{166}Ho and ^{177}Lu are shown in Figures 2.3a and 2.3b, respectively. Both isotopes emit β- particles and γ-rays during decay, making real time imaging during treatment possible. The γ-emission, given by the vertical arrows, can be detected using a gamma detector. β-emission is indicated by the sloping arrows.

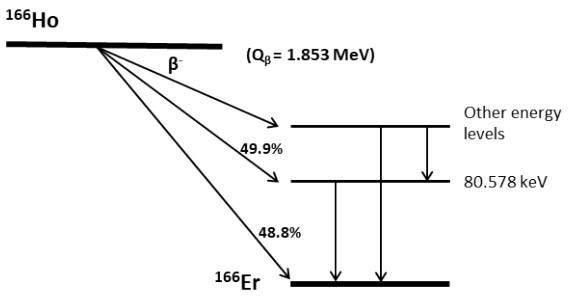

(a) The decay scheme of ^{166}Ho to the stable ^{166}Er based on [29, 30]

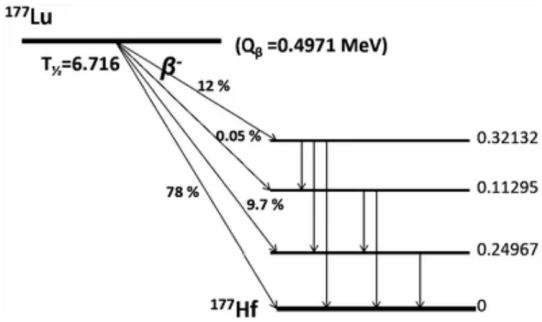

(b) The decay scheme of ^{177}Lu to the stable ^{177}Hf [26].

Figure 2.3: The decay schemes of ^{166}Ho and ^{177}Lu are given, indicating both the emission of β-particles and γ-rays.

2.3. Production routes

Radionuclides can either be produced in a nuclear reactor or in an accelerator. Accelerator produced radionuclides can be made in a linear accelerator or by bombarding the nuclide with a beam, coming from a cyclotron [31]. The benefit of using a cyclotron is that the produced isotope is, in general, another chemical element than the isotopes in the target material. This makes them suitable for chemical or physical separation, which then results in a higher specific activity [32]. In a reactor, neutrons are used to create radionuclides, the following reactions occur in a reactor [33]:

1. Neutron radiative capture (n,γ)
2. Neutron capture followed by particle emission (n,p), (n,α), (n,n')
3. Fission (n,f)

The current production routes of ^{166}Ho and ^{177}Lu are shown in Figures 2.4a and 2.4b, respectively. For both radionuclides a direct and an indirect production route exists [23, 34].

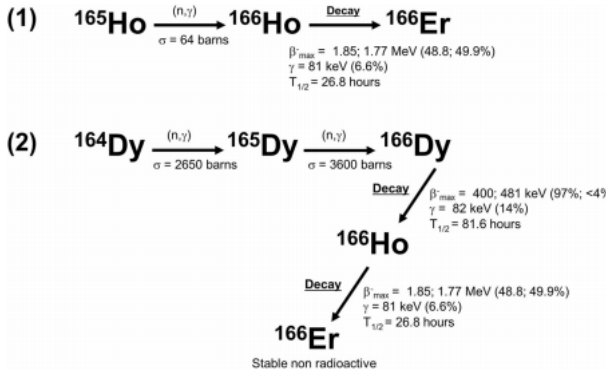

(a) The current direct (1) and indirect (2) production routes of ^{166}Ho, the decay to the stable ^{166}Er is also given [23].

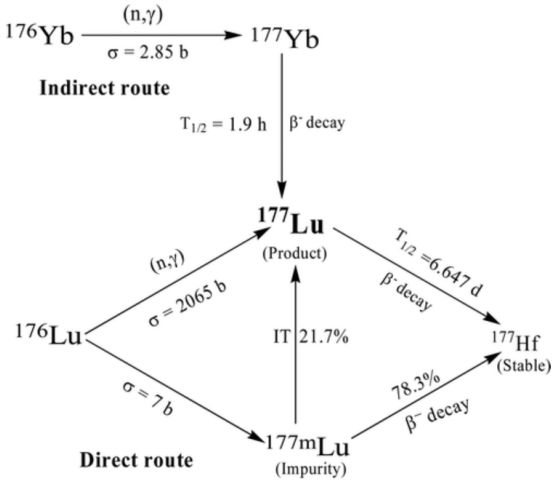

(b) The current indirect and direct production routes of ^{177}Lu [34].

Figure 2.4: The current direct and indirect production routes of ^{166}Ho and ^{177}Lu.

The chance of interaction between the neutron and the target material is given by the cross section σ [b], with [b] indicating the unit barn, which is 10^{-24} cm^2 [33]. The cross section depends on the energy of the incoming neutron. The cross section is higher for neutrons with a lower energy [35]. For the production of medical radionuclides with a (n,γ) reaction the lower energy neutrons, the thermal neutrons and epithermal neutrons, are therefore of importance [36]. The chance of interaction between the target material and the thermal neutron is given by σ_0 [b] and the chance of interaction between the epithermal neutron and the target material is given by I_0 [b], the resonance integral [36]. Both σ_0 and I_0 are used in the calculation of the reaction rate, see equation 2.3.

When activated by a (n,γ) reaction, the only difference between the targeted nuclide and the produced nuclide is the mass of one neutron. This results in chemically very similar characteristics, which makes separation challenging [15]. After irradiation the solution contains not only the produced radionuclide, but also the target material, resulting in a low specific activity. A possibility for making radionuclides with a high specific activity via a (n,γ) reaction is investigated in this thesis. The production method is based on the Szilard-Chalmers effect.

2.4. Szilard-Chalmers effect

The Szilard-Chalmers effect is the mechanism on which the new production route is based. The Szilard-Chalmers effect was discovered in 1934 by L. Szilard and T.A. Chalmers. They discovered that after neutron irradiation of ethyl iodide, an iodine radioisotope could be isolated [10]. This was possible, because after the neutron is captured in the compound, the excess energy is released by emission of a prompt gamma. In this process, recoil energy is emitted, depending on the mass of the radioisotope and the energy of the prompt gamma [12]. When there is a high enough recoil energy, the bond between the target complex and the radioisotope is broken [15]. The radioisotope is emitted in the opposite direction of the prompt gamma, because of conservation of momentum [37]. After the recoil, the radioisotope is in a different chemical state than the target complex. This enables the extraction of the radioisotope and producing a radionuclide with a high specific activity [38].

In order to achieve a high specific activity with the Szilard-Chalmers effect a few conditions have to be satisfied [39]:

1. The bond between the chelator and the produced radionuclide must be broken
2. The produced radionuclide must not recombine with the chelator, which would lead to relabeling
3. The produced radionuclide must not interchange with other inactive atoms
4. It must be possible to separate the produced radionuclide

The, to be investigated, idea is to label the targeting nuclide to a chelator, this compound will be irradiated in the reactor. After the Szilard-Chalmers effect the produced radionuclide will be separated from the chelator, enabling the chemical separation between the targeting nuclide and the produced radionuclide, since the targeting nuclide is still bound to the chelator. A schematic overview of this process is given in Figure 2.5, with lutetium labeled with DOTA (LuDOTA) as the lanthanide-chelator complex.

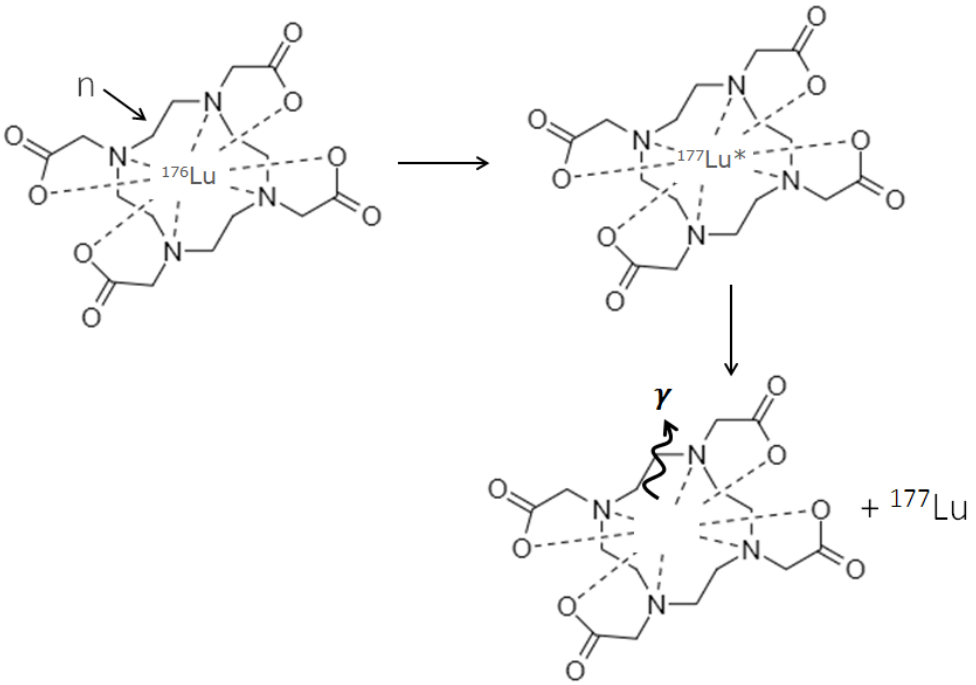

Figure 2.5: A schematic overview of the Szilard-Chalmers effect for ^{176}LuDOTA resulting in activated and from DOTA separated ^{177}Lu due to the energy from the prompt gamma.

2.5. Chelators

Chelators are complexes which can be used to bind to a nuclide. The stability of the chelators depends on whether it is a cyclic or a linear chelator [40]. The stability is given by the stability constant K_{ML}, which is described by equation 2.1 [8], it determines how likely it is that a compound will degrade.

$$K_{ML} = \frac{[ML]}{[M][L]} \text{ for } ML = M + L \tag{2.1}$$

With ML being the concentration of the metal complex, M the concentration of the metal ion and L the concentration of the polydentate chelator. Cyclic chelators are more stable than linear chelators, which makes them more favourable [40]. In this project, a water soluble chelator is needed, since the solvent in the loop will be water based. The solvent will be water based, because of safety regulations. Possible water soluble chelators are: 1,4,8,11-tetra-azacyclotetradecaan (cyclam), 1,4,7,10-Tetraazacyclododecane-1,4,7,10-tetraacetic acid (DOTA), diethylenetriaminepentaacetic acid (DTPA), ethylenedinitrilotetraacetic acid (EDTA) and nitrilotriacetic acid (NTA) [7, 41, 42]. Furthermore, the chelator should not label with the isotope too fast, because this would lead to relabeling before separation is possible. The complex should also remain stable under higher temperatures and gamma radiation. Based on the stability EDTA, DTPA and DOTA are the most promising with the following stability constants for: holmium labeled with EDTA (HoEDTA) $K_{\text{HoEDTA}} = 18.05$, holmium labeled with DTPA (HoDTPA) $K_{\text{HoDTPA}} = 22.78$ and holmium labeled with DOTA (HoDOTA) $K_{\text{HoDOTA}} = 24.5$ [43, 44]. The chemical structure of EDTA, DTPA and DOTA are shown in Figures 2.6a, 2.6b and 2.6c respectively.

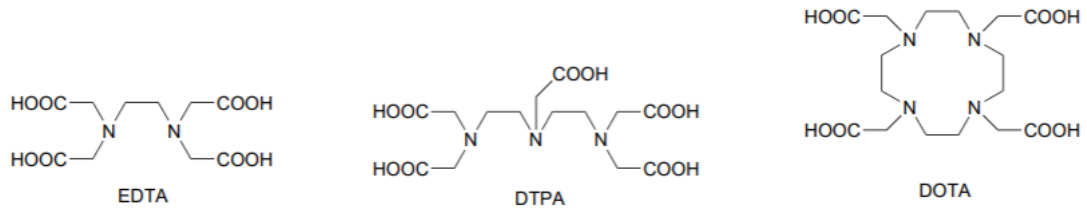

(a) The chemical structure of EDTA.

(b) The chemical structure of DTPA.

(c) The chemical structure of DOTA.

Figure 2.6: An overview of the chemical structure of the chelators EDTA, DTPA and DOTA [45].

2.6. Neutron spectrum

The hot atom production loop will be placed inside the DLDR tube of the Higher Education Reactor (Hoger Onderwijs Reactor or HOR) of the Delft University of Technology. Therefore, for the calculations in this thesis, the neutron flux in the DLDR tube has to be known. The neutron flux in the DLDR tube has been obtained using MCNP 6.1 simulation software [46]. The relative neutron flux as a function of the distance from the middle of the tube is given in Figure 2.7. To obtain the neutron flux [$s^{-1}cm^{-2}$] the relative neutron flux is multiplied with $1.5*10^{17}$ $s^{-1}cm^{-2}$.

The loop is for the purposes of this thesis assumed to be a square with a maximum size of 15x15 cm, since the diameter of the DLDR tube is 15 cm [46]. Because of this, the neutron flux is approximated to be a constant inside the loop. This results in the following fluxes, see Table 2.1. The thermal flux range is up to 0.55 eV, this is the cadmium cut-off energy [36].

Table 2.1: The neutrons fluxes in the DLDR tube of the HOR at the TU Delft [46].

Type of neutrons	flux [$s^{-1}cm^{-2}$]
Thermal neutrons [0 eV - 0.55 eV]	$4.25 * 10^{12}$
Epithermal neutrons [0.55 eV - 100 keV]	$6.69 * 10^{11}$
Fast neutrons [100 keV - 20 MeV]	$5.30 * 10^{11}$
Neutrons at 1 eV	$1.56 * 10^{10}$

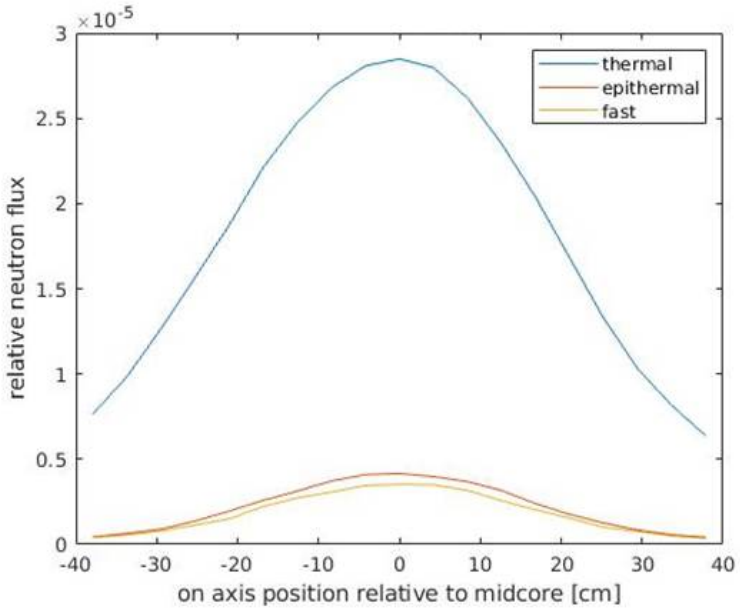

Figure 2.7: The relative neutron flux as a function of the distance from the middle of the tube. To obtain the neutron flux [$s^{-1}cm^{-2}$] multiply the relative neutron flux with 1.5*10^{17} $s^{-1}cm^{-2}$ [46].

The effect of the neutrons is given by the activation rate R_A [s^{-1}], which is given by equation 2.2 [36].

$$R_A = \int_0^\infty \Phi(v)\sigma(v)\,dv = \int_0^\infty \Phi(E)\sigma(E)\,dE \tag{2.2}$$

With Φ [$s^{-1}cm^{-2}$] the neutron flux and σ [b] the capture cross section. The integral can be divided into integrals over the thermal, epithermal and fast neutrons. This derivation is done by Blaauw et al. [36], by ending with the Høgdahl convention, this results in the following reaction rate.

$$R_A = \sigma_0\Phi_0 + I_0\Phi_e \tag{2.3}$$

Here σ_0 [b] is the thermal capture cross section at 0.025 eV, Φ_0 [$s^{-1}cm^{-2}$] the thermal flux, I_0 [b] the resonance integral and Φ_e [$s^{-1}cm^{-2}$] the epithermal flux at 1 eV. The values for σ_0 and I_0 can be found in tables and literature, such as the literature by De Corte [47]. The values for ^{165}Ho and ^{176}Lu are given in Table 2.2.

Table 2.2: The thermal cross section σ_0 [b] and resonance integral I_0 [b] values for ^{165}Ho and ^{176}Lu [47].

	σ_0 [b]	I_0 [b]
^{165}Ho	58	632
^{176}Lu	2065	1087

2.7. The Hot Atom Loop

In this section an overview is given of the loop-based production method, which can increase the specific activity of radionuclides produced via a (n,γ) reaction. A schematic overview of the loop is given in Figure 2.8. In this schematic overview, lutetium is the addressed element and DOTA the used chelator. The lanthanide-chelator complex goes into the loop, which is placed close to the reactor core. The neutrons from the reactor core initiate the Szilard-Chalmers effect, resulting in a bond rupture between the excited isotope, the produced radionuclide, and the chelator. Then the produced radionuclide (i.e. ^{177}Lu) is separated from the lanthanide-chelator complexes. The produced radionuclide can be extracted from the loop. Because of the loop system, this activation and extraction is a continuous process. The fast extraction is needed to have a low possibility of relabeling, which would result in ^{177}LuDOTA. If the isotope relabels with the chelator, extraction is not possible anymore. Besides the neutrons, also γ-radiation comes from the reactor core. This

γ-radiation can lead to a bond rupture between the target material (i.e. ^{176}Lu) and the chelator, this is called radiolysis. Due to radiolysis the specific activity will be lower, because the target material will be extracted with the produced radionuclide.

As can be seen in Figure 2.8, it is possible to close the small loop, that is close to the reactor core. Because of this, it is also possible to have multiple rounds of irradiation before the extraction takes place. It will be investigated whether, it is beneficial to have multiple rounds of irradiation before extraction takes place. This will depend on how fast the produced radionuclide relabels and what the effect of the radiolysis is. For correct functioning of the loop, the following requirements have to be investigated:

1. Labeling
2. Stability
   (a) Time and temperature
   (b) Gamma radiation
3. Szilard-Chalmers reaction
4. Extraction

These requirements are further explained in the subsections 2.7.1-2.7.4. Except for the Szilard-Chalmers effect, the requirements will be experimentally investigated. The experimental investigation of the Szilard-Chalmers effect was not possible, because the HOR was not operating at the time of this thesis. The results from these experiments can be used to determine the theoretical specific activity that can be achieved in the loop.

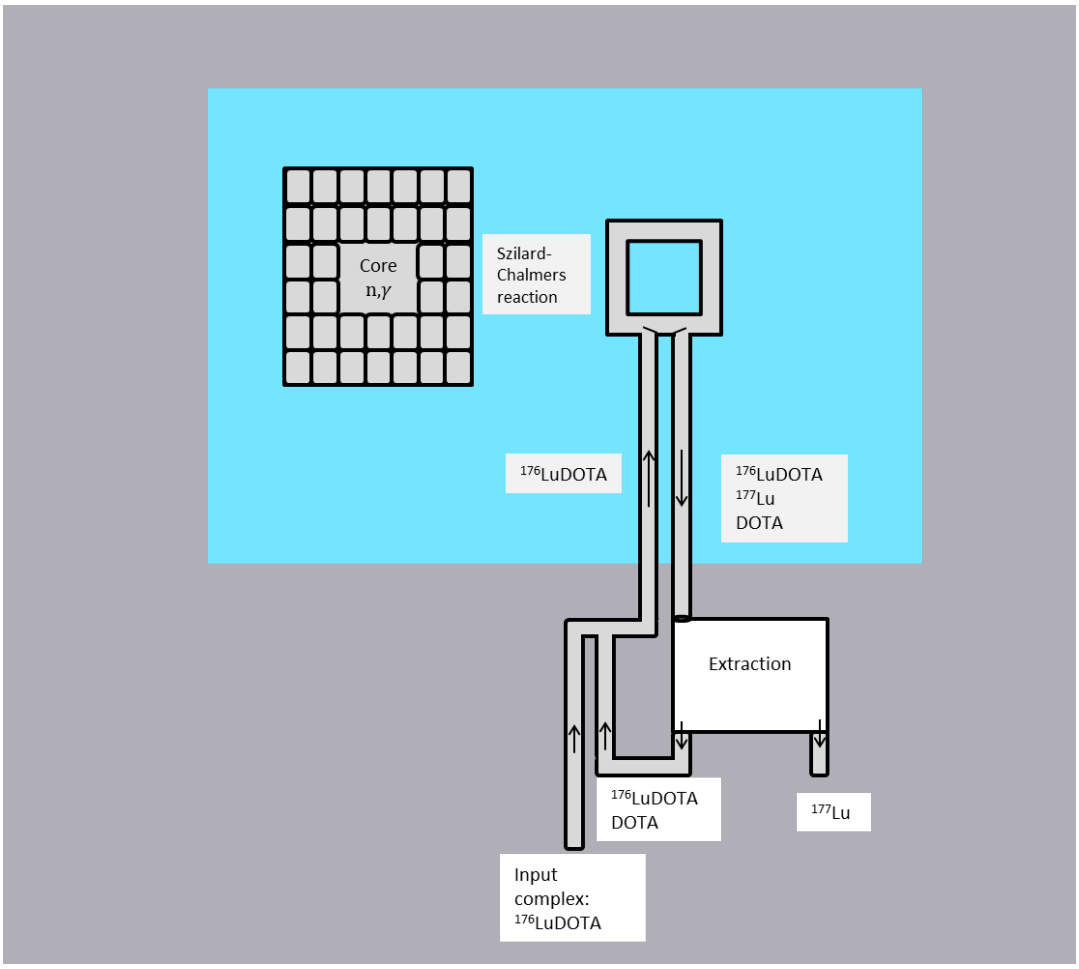

Figure 2.8: A schematic overview of the hot atom loop. The blue background indicates the swimming pool around the reactor core. Grey was chosen as background colour for better contrast.

The loop is called 'The Hot Atom Loop', because hot atoms are formed during the (n,γ) reaction. Hot atoms are atoms "in an excited energy state or having kinetic energy above the ambient thermal level, usually as a result of nuclear processes" [48].

2.7.1. Labeling

The target nuclide and the chelator have to be labeled. Usually this is done at higher temperatures, e.g. the protocol for labeling LuDOTA is 30 minutes at 90°C [25], for labeling lutetium with EDTA (LuEDTA) the protocol is 15 minutes at 45°C [49] and for labeling lutetium with DTPA (LuDTPA) the protocol is 15 minutes at 90°C [50]. An optimum has to be found to label all the nuclides with the least amount of chelators. Aiming for an ideal ratio of element:chelator of 1:1, because then there are less chelators that could lead to relabeling. Due to the heat coming from the reactor core, the temperature inside the loop will likely be 40°C. Therefore, labeling should not happen too fast at 40°C, because fast labeling at 40 °C, can lead to fast relabeling. As a result of this, the unchelated produced radionuclide (i.e. ^{177}Lu) could label again with DOTA, before the extraction takes place. Once it has relabeled it is not possible anymore to extract the produced radionuclide.

2.7.2. Stability

After labeling, the target material goes into the loop. The temperature in the loop is likely 40°C, therefore the stability of the complex has to be known at this temperature. Another factor affecting the stability is the γ-radiation from the reactor core. This radiation can break the bonds between the chelator and the target material or between different parts of the chelator [14]. To see if parts of the bonds between different parts of the chelator are broken, proton nuclear magnetic resonance (NMR) experiments can be done. For more information about NMR see Clayden et al. [51].

If due to the γ-radiation the target material is released from the chelator, this will lower the maximum achievable specific activity. The SA will be lower, because it is not possible to extract the unchelated activated radionuclide from the unchelated target material. This is because, both nuclides are of the same element and therefore chemical separation is nearly impossible. The gamma dose rate coming from the reactor core is 265 kGy/h [13]. An option to lower the amount of γ-radiation is by shielding the loop, this has been studied for the HOR in the flexible irradiation facility (Flexibele Bestralings Faciliteit or FlexBeFa), the lead shielding from the FlexBeFa results in a gamma dose rate which is 6.3 times lower with the same neutron flux [52].

2.7.3. Szilard-Chalmers effect

The theory behind the Szilard-Chalmers effect has already been explained in section 2.4. The neutron interaction needed for Szilard-Chalmers has been explained in section 2.6. Due to the Szilard-Chalmers effect there will be unchelated radionuclides (i.e. ^{177}Lu) and DOTA in the loop. The radionuclides are extracted in the extraction step. The unlabeled DOTA remains in the loop. The amount of unlabeled DOTA will be determined, to determine whether it is necessary to have an extra step in the loop for relabeling this DOTA. If there is an excess of free DOTA, this increases the chance of relabeling. This can be prevented by adding an extra step, after the extraction, where the free DOTA is labeled with new target material.

2.7.4. Extraction

An extraction method is liquid-liquid extraction, enabling a constant production process. Another extraction method is ion exchange extraction, which can be done using Dowex resins [25]. A cation exchange resin can be used to adsorb the cations (i.e. $^{177}Lu^{3+}$), where the anions (i.e. $^{176}LuDOTA^{-}$ [53]) remain in the liquid phase [54]. When washing the resins with a high molarity of hydrochloric acid (HCl), $^{177}Lu^{3+}$ will be adsorbed in the HCl and can be eluted [55]. Depending on the effects of the gamma radiation and the relabeling, the extraction can be done after a certain amount of irradiation rounds or after each round. The batches that are extracted during the irradiation will be collected on the column with the resins.

2.8. Specific activity calculations

The radioactivity gives the amount of decayed radionuclides. The expressions for the activity are given by equation 2.4 [56].

$$\begin{aligned} A(t) &= -\frac{dN(t)}{dt} = \lambda N(t) \\ A(t) &= A(0)e^{-\lambda t} \end{aligned} \tag{2.4}$$

Where $A(t)$ [Bq] is the activity at time t. $A(0)$ [Bq] the activity at a known moment $t = 0$. $N(t)$ is the number of unstable nuclei, t [s] is the decay time and λ [s^{-1}] the decay constant . The decay constant λ depends on the half-life $t_{\frac{1}{2}}$ [s], the time in which the activity has become half of the original value. This relation is given by equation 2.5.

$$t_{\frac{1}{2}} = \frac{\ln(2)}{\lambda} \tag{2.5}$$

To determine the possible achievable specific activity with the loop-based production method, the equation for the specific activity has to be known. The general equation for the specific activity is given in equation 2.6, taking into account the decay of the product during the irradiation [26]. The capture cross section is assumed to follow the $\frac{1}{v}$ law. The activation rate, R_A [s^{-1}] is the activation rate from equation 2.3, taking into account both the thermal and epithermal excitation.

$$SA = \frac{A(t)}{m_{tot}} = \frac{\lambda N(t)}{m_{tot}} = \frac{N_0 R_A}{m_{tot}} * (1 - e^{-\lambda t}) \tag{2.6}$$

With N_0 the initial target atoms, m_{tot} [g] the total mass of all the nuclides and t [s] the irradiation time. N_0 can be calculated as given in equation 2.7.

$$N_0 = N_A * V * M * h \tag{2.7}$$

With N_A [atoms/mol] being Avogadro's number, V [L] the target volume, M [mol/L] the molarity of the target material and h the isotopic abundance. The equations for the specific activity in the loop, taking into account the Szilard-Chalmers effect are based on the equations from Zhernosekov et al. [14]. The specific activity when taking into account the Szilard-Chalmers effect is given in equation 2.8.

$$SA_{sz} = \frac{A_{sz}}{m_{SA}} = \frac{\lambda N_{sz}}{m_{SA}} \tag{2.8}$$

Here m_{SA} [g] is the mass specific for this situation, which is explained further in equation 2.10. N_{sz} is the number of uncomplexed activated radionuclides (i.e. ^{166}Ho), the produced radionuclides. N_{sz} can be calculated with the formula for N^*_{SC} in the paper from Zhernosekov et al. this is given in equation 2.9.

$$N_{sz} = N^*_{SC} = \frac{R_A N_0 (1 - F)}{\lambda}(1 - e^{-\lambda t}) \tag{2.9}$$

F is the fraction of produced radionuclides retained in the complex (i.e. ^{166}HoDOTA). Equation 2.10 expresses the division of the mass and which fraction is needed for the specific activity calculation.

$$\begin{aligned} m_{tot} &= m_1 + m_2 + m_3 + m_4 \\ m_{SA} &= m_1 + m_3 = (f_r + f_{SZ}) * m_{tot} \end{aligned} \tag{2.10}$$

The masses with different subscripts are: m_1 [g] is the separated target material (i.e. ^{165}Ho) due to radiolysis, m_2 [g] is the target material retained on the complex (i.e. ^{165}HoDOTA), m_3 [g] is the recoiled produced radionuclide (i.e. ^{166}Ho), due to the Szilard-Chalmers effect and m_4 [g] is the relabeled produced radionuclide (i.e. ^{166}HoDOTA). m_{SA} exists only of the masses of the radiolysed target material and the recoiled produced radionuclide, since it is assumed that total separation of the complexed and not complexed isotope is possible. f_r gives the fraction of radiolysed target material and f_{SZ} the fraction of recoiled produced radionuclides due to the Szilard-Chalmers effect. A final equation for the specific activity, when taking into account the Szilard-Chalmers effect is given in equation 2.11.

$$SA_{sz} = \frac{(\sigma_0 \Phi_0 + I_0 \Phi_e) N_0 (1 - F)(1 - e^{-\lambda t})}{(f_r + f_{SZ}) * m_{tot}} \tag{2.11}$$

2.9. Instant thin layer chromatography

Instant thin layer chromatography (iTLC) is a separation method, using a strip (the stationary phase) and a liquid (the mobile phase). iTLC can be used to determine the radiochemical purity of a sample, the amount of the sample in the desired radiolabeled form. Usually the stationary phase is a strip of silica gel or polysilicic acid [57]. A drop of the sample, containing a radioactive tracer (i.e. ^{177}Lu), is applied to the strip after which the strip is placed in the developing chamber, which contains a small layer of the mobile phase. The mobile phase will go up the strip, due to capillary forces. The compounds having more affinity with the stationary phase will stay behind, whereas the compounds having affinity with the mobile phase will move upwards, separating the different compounds [58]. The strip should be placed in the mobile phase in such a way that the sample is above the mobile phase, in order to not contaminate the sample. A schematic overview of this is given in Figure 2.9.

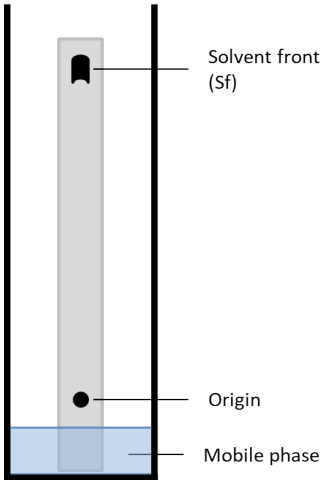

Figure 2.9: A schematic overview of the working of iTLC strips.

It is of importance to have a clear distinction between the spots belonging to the different compounds. The solvent front (Sf) must remain beneath the end of the strip. Once taken out, the strip must be dried, after which the placement of the activity on the strips can be made visible using a phosphor imager. The distance traveled by the compounds is given by the R_f value which is defined as given in equation 2.12, which is a value between 0 and 1 [59].

$$R_f = \frac{\text{Distance between the sample and the origin}}{\text{Distance between the Sf and the origin}} \tag{2.12}$$

To determine the ratio of the different components, the strip can be imaged or cut, in two or more parts if there are more than two different components and corresponding dots. The activity on the different parts of the strips can be measured using a gamma counter.

3

Methods and Materials

In this chapter the methods and materials are explained. The neutron activation will be investigated computationally, since the HOR was not operating during the time of this thesis. More iTLC-based separation methods have been investigated than the method described in this chapter. Those protocols are not described here, because the protocols did not give a consistent separation. The ratios of the nuclide compared to the chelator in the samples is given by (nuclide:chelator) in front of the sample.

3.1. Materials

MilliQ water (MQ), EDTA, DTPA and TLC silica gel strips 60 F254 from Merck (Darmstadt, Germany). DOTA was purchased from Chematech (Dijon, France). Sodium acetate anhydrous >99%, holmium(III) chloride hexahydrate, sodium hydroxide, deuterium oxide 99.9%, Dowex 50WX8 50-100 mesh hydrogen form resins and ammonium acetate (NH_4Ac) from Sigma Aldrich (Zwijndrecht, The Netherlands). Acetonitrile chromasolv for HPLC far UV, acetone, methanol and acetic acid from Honeywell (Seelze, Germany), ammonium hydroxide solution and sodium chloride from J.T. Baker (Roskilde, Denmark). HCl 30%, PS semi-micro cuvettes 340-900 nm, 2 mL sample vials and 20 mL sample vials from VWR International BV (Amsterdam, the Netherlands) and lutetium(III) chloride hexahydrate from ABCR (Karlsruhe, Germany). The iTLC silica gel impregnated strips were purchased from Agilent Technologies (Amstelveen, the Netherlands) and ^{177}Lu was received from the Erasmus Medical Centre (Rotterdam, the Netherlands), in HCl pH 2 solution. 50 mL plastic tubes and 1.5 mL Eppendorf vials were purchased from Sarstedt (Nümbrecht, Germany). 4 mL sample vials from Roth (Karlsruhe, Germany) and NMR tubes from Norell (Saint-Aubin, France).

The following equipment was used: A thermoshaker from Labnet International, Inc (Edison, USA). A Packard cyclone storage phosphor system and a Wallac Wizard 2 3" Automatic Gamma Counter, for which a lutetium specific protocol was made, from Perkin Elmer (Rotterdam, The Netherlands). An UV-6300PC Double Beam spectrophotometer from VWR International bv (Amsterdam, the Netherlands). A princeton gamma tech model LG22 germanium detector from EG&G ORTEC (Meerbusch, Germany). A 744 pH Meter from Metrohm (Barendrecht, the Netherlands) and PEHANON pH paper, numbers 904 : 11, 13, 15, 16, 17, 20 and 21 from Machery-Nagel (Düren, Germany). Freezdrier EZ-DRy from KINETICS (Bangkok, Thailand), a 400-MR DD2 NMR spectrometer from Agilent Technologies (Amstelveen, the Netherlands) and a GC220 ^{60}Co gamma source with a dose rate of 0.59 kGy/h.

3.2. Labeling holmium

The following protocol was used to determine the labeling of holmium with the chelators. In the protocol the parameter *C* was used for DOTA, DTPA and EDTA. The buffer was a 1 M sodium acetate acetic acid pH 4.3 buffer. The following samples were made: a holmium sample (1 mL 10 mM Ho and 1 mL buffer), the chelator samples (1 mL *C* and 1 mL buffer), the samples containing holmium and the chelator (1:10000)Ho:*C* (0.5 mL 10 mM *C*, 0.5 mL 1 μM Ho and 1 mL buffer) and (1:1)Ho:*C* (0.5 mL 10 mM *C*, 0.5 mL 1 mM Ho and 1 mL buffer). The HoDOTA and HoDTPA samples were stirred at 300 rounds per minute (rpm) for 15 minutes at 90°C in the thermoshaker. HoEDTA samples were stirred at 300 rpm for 15 minutes at 45°C in the thermoshaker. The samples were placed in a cuvette for the measurement with the spectrophotometer. Furthermore, two cuvettes were filled with 2 mL MQ. First a background measurement was done with the two MQ samples. Then the other samples were measured, with a MQ sample as reference.

3.3. Labeling lutetium

3.3.1. iTLC

To determine the labeling of lutetium, first the mobile phase and stationary phase for the iTLC were determined. The mobile phase was 5% acetonitrile and the stationary phase was an iTLC silica gel strip. Two samples were used to determine whether the separation was possible, one with only Lu (120 μL buffer, 25 μL 1 mM Lu_3Cl and 2 μL ^{177}Lu (20 kBq)) and the other with (1:10000)LuDOTA (120 μL buffer, 25 μL 1 μM Lu_3Cl, 25 μL 10 mM DOTA and 2 μL ^{177}Lu (20 kBq)). An excess of DOTA was added, to be sure, that all the lutetium will be labeled. The labeling was done by stirring (1:10000)LuDOTA at 300 rpm for 15 minutes at 90°C in the thermoshaker. Radioactive ^{177}Lu was used as a tracer, which was visualised with the phosphor imager.

To determine the labeling percentage iTLC was used. The iTLC strips were cut in pieces of 15 cm x 0.8 cm. For the mobile phase 5% acetonitrile was used. 5 μL of the sample was applied 2 cm from the bottom and placed in the developing chamber for 9 minutes. After this the strip was dried by air for 30 minutes and then packed in duct-tape to prevent radioactive contamination. The spotting and developing of the samples are shown in Figures 3.1a and 3.1b.

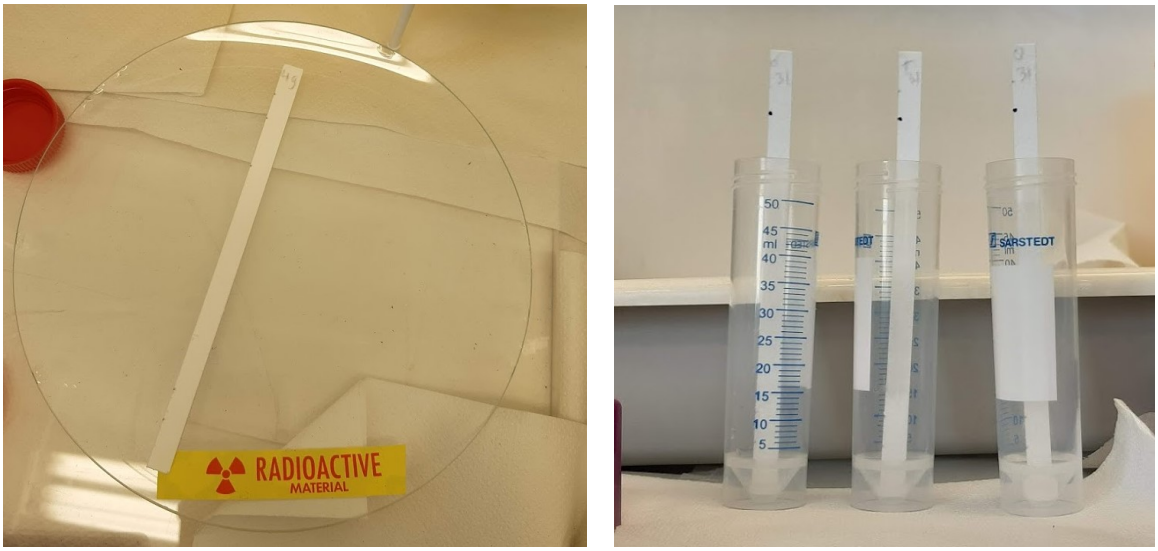

(a) The setup to apply the sample on the iTLC strip.

(b) The chambers to develop the iTLC strip.

Figure 3.1: The setup to measure the labeling percentage by using iTLC.

After this the development on the iTLC strip was either made visible using the phosphor imager or the activity was measured using the Wallac gamma counter. To use the phosphor imager, first the phosphor plate was cleaned by exposure to the lamp for 30 minutes. Then the plate was exposed to the radioactive iTLC strip for 15 minutes. For this the plate was placed inside the cassette, together with the iTLC strips, to prevent contamination from light. After this an image was created using the phosphor imager. This setup is shown in Figure 3.2.

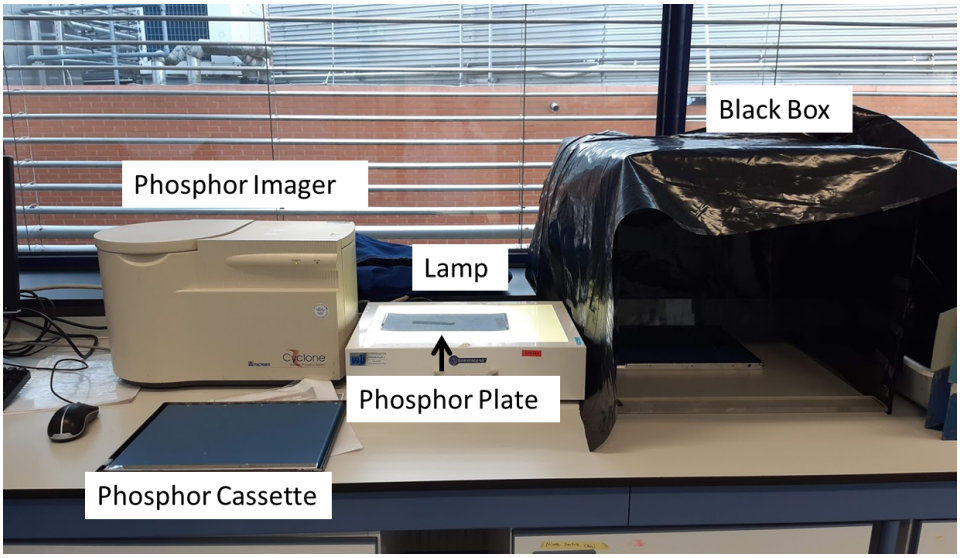

Figure 3.2: The phosphor imager setup. Showing the lamp to clean the phosphor plate, the phosphor plate itself, the phosphor cassette, the black box and the phosphor imager to create the image.

To determine the labeling percentage the strip was cut at 11 cm from the bottom, resulting in two separate parts. These parts are placed in different counting vials. Those vials were measured using the Wallac gamma detector, this is illustrated in Figures 3.3a and 3.3b. The labeling percentage can be determined with equation 3.1.

$$\text{LuDOTA} = \frac{\text{A}_{\text{above}}}{\text{A}_{\text{above}} + \text{A}_{\text{below}}} * 100\% \tag{3.1}$$

LuDOTA [%] gives the labeling percentage, A_{above} [Bq] the activity on the upper part of the iTLC strip and A_{below} [Bq] the activity on the lower part of the iTLC strip.

(a) The cut iTLC strips in different counting vials.

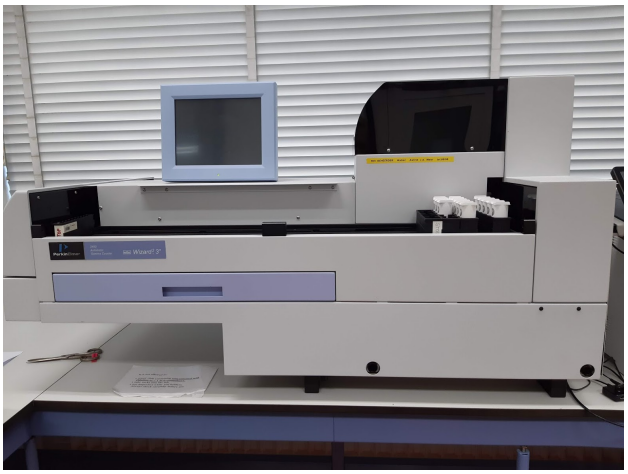

(b) The Wallac gamma detector.

Figure 3.3: The setup to measure the activity on the top and the bottom of the iTLC strip with the Wallac gamma detector.

3.3.2. Temperature and ratio

The labeling efficiency was determined for different temperatures and for different ratios of Lu : DOTA. Solutions of different concentrations of Lu_3Cl and DOTA were made, being: 1, 2, 3 and 10 mM. The samples contained 120 μL buffer, 25 μL X mM Lu_3Cl, 25 μL Y mM DOTA and 2 μL ^{177}Lu (20 kBq), the X and Y indicating the variable concentrations. To determine the labeling of the isotope with the chelator at a certain temperature, the thermoshaker was set to a that temperature for 15 minutes and 300 rpm. The temperatures that were measured are: 20°C, 30°C, 40°C, 50°C, 60°C, 70°C, 80°C and 90°C.

3.3.3. Solvent

The time dependence of the labeling at 40°C, was determined by making (1:1)LuDOTA (120 μL buffer, 25 μL 1 mM Lu_3Cl, 25 μL 1 mM DOTA and 2 μL ^{177}Lu (20 kBq)). The thermoshaker was set on 40°C for 15 minutes at 300 rpm. The labeling percentage was determined after 1, 3, 5, 10 and 15 minutes.

3.4. Stability lutetium

3.4.1. Time and temperature

(1:1)LuDOTA (100 kBq) was placed in the thermoshaker at 40°C. The labeling percentage was measured after 0.5, 1, 2, 4, 24, 72, 168 and 504 hours. The percentage of complexed versus uncomplexed lutetium was determined by measuring the iTLC strips with the Wallac. The same experiment was done, with the samples at room temperature (RT), 20°C, to determine the effect of time on the stability. The samples at RT were not in a thermoshaker.

3.4.2. Gamma radiation iTLC

Radioactive (1:1)LuDOTA samples were made by adding 25 μL 10 mM DOTA, 25 μL 10 mM Lu and 120 μL buffer and 2 μL of ^{177}Lu (300 kBq) as a tracer. The samples were left at 90°C for 15 minutes for the labeling. The percentage of complexed versus uncomplexed lutetium of the samples was determined, by measuring the iTLC strips with the Wallac. After this the samples were placed inside the ^{60}Co source, to be irradiated. The samples were measured after 0, 68, 163 and 330 h. For each time the percentage of complexed versus uncomplexed lutetium was measured again to determine the effect of the gamma radiation.

3.4.3. Gamma radiation NMR

The non radioactive (1:1)LuDOTA samples were made by adding 250 μL 10 mM DOTA, 250 μL 10 mM Lu and 1 mL buffer. The samples were left at 90°C for 15 minutes at 300 rpm for the labeling. One sample was placed inside the ^{60}Co source, to be irradiated with 298.5 kGy. The other sample, the reference sample, which was left under the same conditions, except for the gamma radiation. Also reference samples containing only Lu, DOTA and the sodium acetate acetic acid buffer were made. The samples were freeze dried overnight at -50°C, see Figure 3.4a. After the liquid had evaporated, the samples were put in the NMR tubes and dissolved using 330 μL D_2O, see Figure 3.4b. The samples were measured with H-NMR at 399.7 MHz.

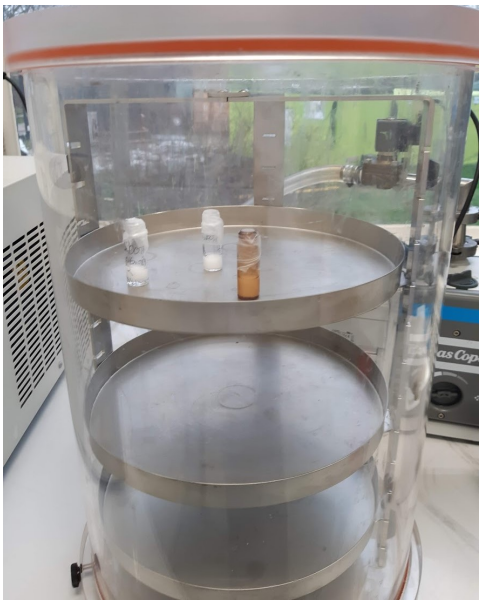

(a) Samples inside the freeze drier.

(b) The samples in the NMR tubes, dissolved in D_2O

Figure 3.4: Preparation of the NMR samples. First the samples were freeze dried, then the samples were put in the NMR tubes and dissolved in D_2O.

3.5. Extraction lutetium

First the pH dependence of the attachment of free lutetium and LuDOTA to the resins was determined. For this the procedure was the same for all the different pH values, only varying the pH of the HCl solution, therefore pH X will be used in the protocol as a parameter. 15 mg of the Dowex resins was placed in an Eppendorf vial. The resins were activated by washing with 200 μL MQ for 5 minutes at 20°C and 1000 rpm, in the thermoshaker. Then washed with 200 μL pH X also 5 minutes at 20°C and 1000 rpm. 550 μL pH X HCl solution, 120 μL pH 4.3 HCl solution, 25 μL 1 mM Lu_3Cl and 5 μL ^{177}Lu (20 kBq) were added to the resin and stirred for 10 minutes 5 minutes at 20°C and 1000 rpm in the thermoshaker. After which 600 μL was pipetted in an Eppendorf, Eppendorf 1 in Figure 3.5. The resins with 100 μL of the solution remained in the other Eppendorf vial, Eppendorf 2, as shown in Figure 3.5. The activity of both Eppendorf vials was measured with the Wallac gamma detector. The activity on the resins and the activity in the liquid phase was determined with the following equations 3.2. The visual explanation of A_1, A_2, A_3, V_1 and V_2 is given in Figure 3.5.

$$\begin{aligned} A_2 &= A_1 * \frac{V_2}{V_1} \\ A_{liq} &= A_1 + A_2 \\ A_{res} &= A_3 - A_2 \end{aligned} \tag{3.2}$$

To validate the extraction method, partly labeled lutetium is extracted. This is determined by the extraction of (3:1)LuDOTA with the Dowex resins, the resins were washed with 200 μL MQ, 5 minutes at 20°C and 1000 rpm and the same procedure with 200 μL 10^{-5} M HCl solution. Then the (3:1)LuDOTA (120 μL pH 4.3 HCl solution, 25 μL 3 mM Lu_3Cl, 25 μL 1 mM DOTA, 5 μL ^{177}Lu) was labeled by stirring at 300 rpm for 15 minutes at 90°C. 525 μL 10^{-5} M HCl solution was added to the Eppendorf vial together with the (3:1)LuDOTA, the total volume being 700 μL. The solution was mixed for 20 minutes at 20°C and 1000 rpm. After which 600 μL was pipetted in an Eppendorf vial, Eppendorf 1. The resins with 100 μL of the solution remained in the other Eppendorf vial, Eppendorf 2. The activity was measured with the Wallac gamma detector. The 100 μL was pipetted out of the Eppendorf vial containing the resins, 700 μL 4 M HCl solution was added. The Eppendorf vial was again mixed for 20 minutes at 20°C and 1000 rpm after this 600 μL was placed in a new Eppendorf vial 1. The activity in both Eppendorf vials was measured again. For the activity on the resins and in the liquid phase, equation 3.2 can be used. If the liquid contained 1 M HCl or a higher amount of HCl, the vials were measured using the germanium detector, since this was not allowed with the Wallac gamma detector.

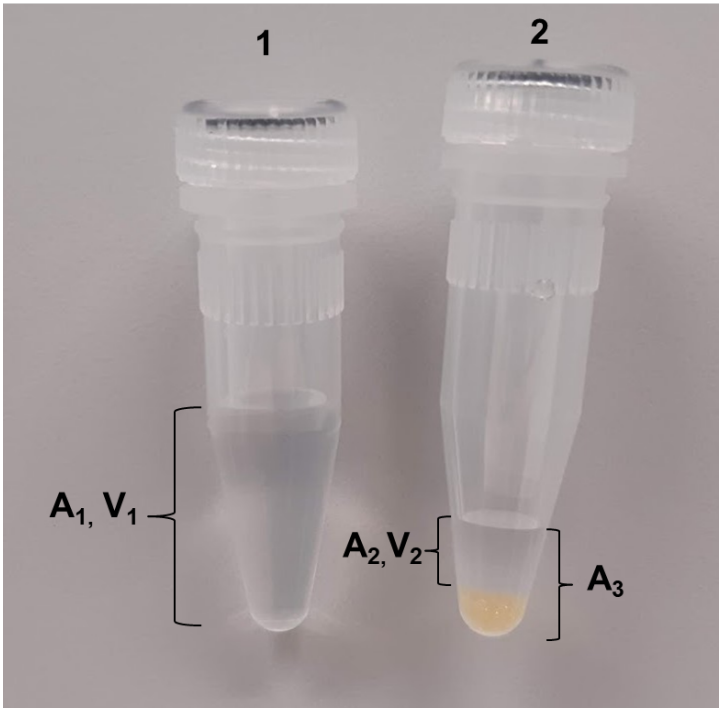

Figure 3.5: The separated liquid phase (left) and the resin phase (right).

3.6. Theoretical specific activity

The effect of the Szilard-Chalmers reaction and the Szilard-Chalmers reaction with loop-based production, was modeled using a Python script. The setup for the simulation is given in the block scheme in Figure 3.6. The input variables are the volume, the total irradiation time, t_{irr}, the number of rounds before extraction, R_e, and the constants, such as the half-life and the neutron flux.

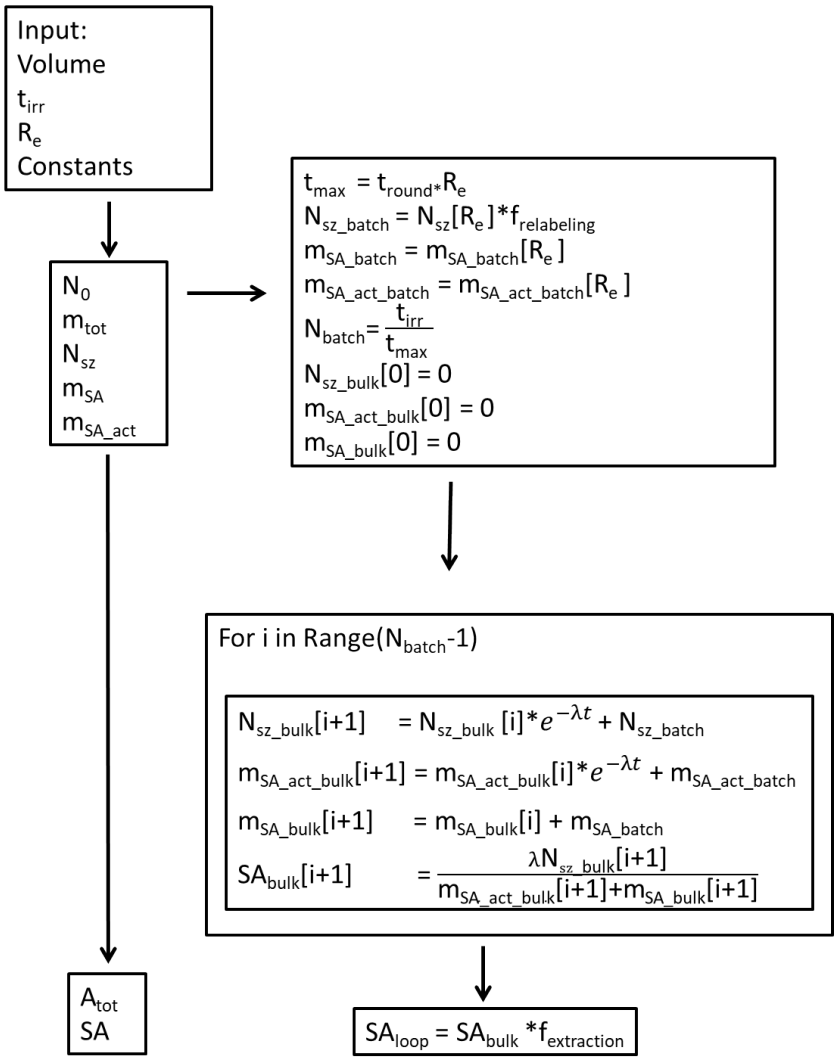

Figure 3.6: A block scheme of the used Python script.

With the input variables the number of target nuclides, N_0, the mass of the target material, m_{tot}, the irradiation time of one batch, t_{max} and the number of activated and recoiled radionuclides, N_{sz} are calculated. N_{sz} is calculated using equation 2.11. Also the mass of the radiolysed target material, m_{SA} and the mass of the recoiled activated radionuclides, m_{SA_act} are calculated, these are fraction of the m_{tot}. From this the activity, A_{tot}, and the specific activity, SA, are calculated as a function of the irradiation time. Furthermore, the calculations for in between extraction are done. To determine the effect of in between extraction, N_{sz}, m_{SA} and m_{SA_act} are determined for one batch. The batches indicate the extraction during irradiation. Based on these extractions the bulk can be determined, this is what remains on the column, where the batches are collected in the case of ion exchange extraction. The decay of the previous batches is accounted for in the calculation of the bulk, also in the m_{SA_act}, because the decay products can be chemically separated. The extraction of the batches is repeated for the total amount of batches, N_{batch}, which depends on the total irradiation time and the irradiation time of one batch. SA_{bulk} is the specific activity on the column. The part of the activated isotope that cannot be eluted, $f_{extraction}$, is accounted for in the calculation of the final specific activity, SA_{loop}.

4

Results and Discussion

In this chapter the results of the experiments are shown and discussed. The error bars were calculated using the standard deviation, based on at least three measurements. Some error bars are too small to be visible in the figure. The results are given in the same order as the methods were explained. First the results of the experimental data for the requirements of the loop are given and discussed. This data is used in the calculations of the possible specific actitivity.

4.1. Labeling holmium

Holmium-chelator complexes were measured with a spectrophotometer, the chelators being DOTA, DTPA and EDTA. This was done to determine whether it was possible to measure these complexes with a spectrophotometer. For each different chelator a measurement has been done for a (1:10000) Ho:chelator complex and a (1:1) Ho:chelator complex. The (1:10000) Ho:chelator complex should represent 100% labeling, since there is an excess amount of chelator present. In order to be able to conclude something about the labeling, the Ho:chelator complexes should give a deviating peak, a peak at a different wavelength, than the peaks from holmium or the chelator. This peak then corresponds with the holmium-chelator complex.

The results of the labeling experiments of holmium with the chelators are given, HoDOTA in Figure 4.1a, HoDTPA in Figure 4.1b and HoEDTA in Figure 4.1c. The results have been obtained by subtracting the background measurement, of MQ with MQ.

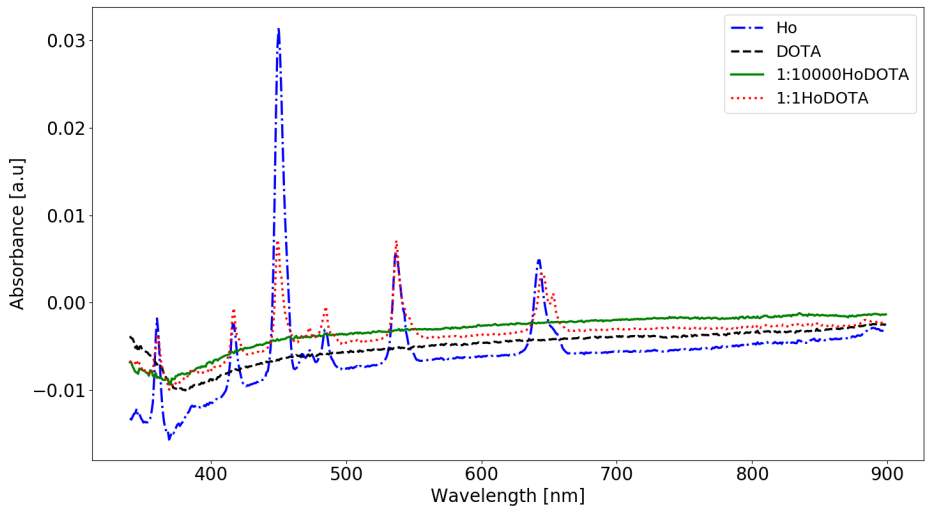

(a) The absorbance spectrum of 10 mM Ho, 10 mM DOTA, (1:10000)HoDOTA complex and (1:1)HoDOTA complex.

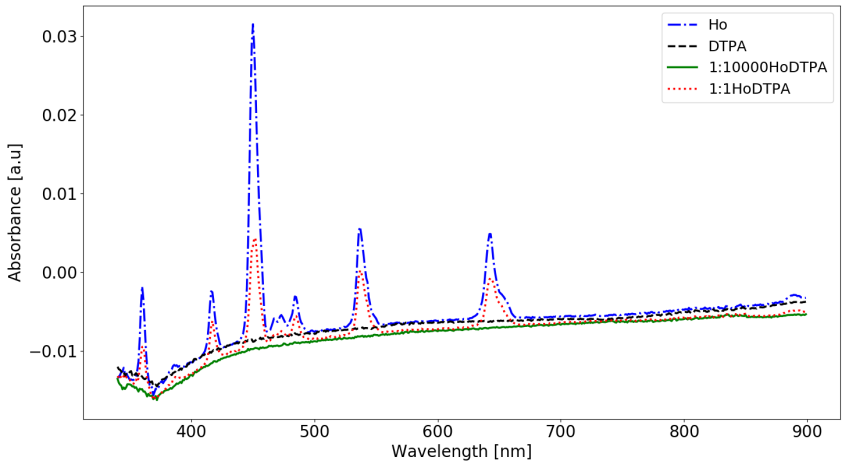

(b) The absorbance spectrum of 10 mM Ho, 10 mM DTPA, (1:10000)HoDTPA complex and (1:1)HoDTPA complex.

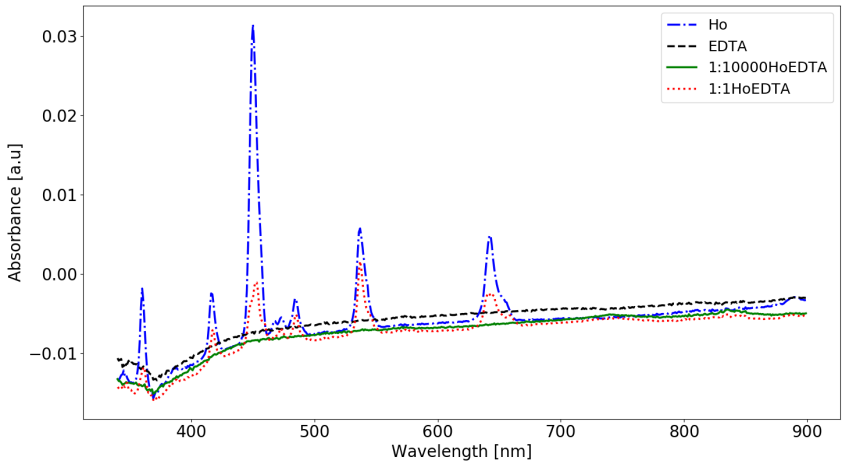

(c) The absorbance spectrum of 10 mM Ho, 10 mM EDTA, (1:10000)HoEDTA complex and (1:1)HoEDTA complex.

Figure 4.1: The absorbance results of the measurements with the spectrophotometer.

As can be seen in Figures 4.1a-4.1c, in each of the measurements there was an absorbance spectrum present for the 10 mM Ho sample, while none of the chelators show an absorbance spectrum. The (1:1) Ho:chelator complexes do show an absorbance spectrum. This spectrum shows absorbance peaks at the same wavelength as the holmium sample. The holmium peaks were expected to be at: 345, 361, 385, 416, 451, 485, 536 and 640 nm, with the peaks at 345 and 385 nm being low compared to the other peaks [60]. These wavelengths correspond with the wavelengths that were obtained during the measurements with the spectrophotometer. For the chelators no absorbance spectra were found in the literate. For DTPA it was even found in the literature that it would not show an absorbance spectrum [61]. The (1:10000)complexes do not show an absorbance spectrum. There are also no peaks visible that corresponds to the peaks of holmium, this could be because the concentration of holmium is too low to be measured [62]. Since there are no deviating peaks in the (1:10000)complexes, there is no peak that corresponds to 100% labeling. For the (1:1) complexes there was also not a deviating peak that could be used as an indicator for the labeling. Therefore, it was not a feasible method to use to determine the labeling of the complex.

Because it is not possible to draw conclusions about the labeling when using the spectrophotometer and there was no radioactive holmium available, the rest of the experiments were performed using lutetium. Lutetium is a promising element, because of its high cross section. Since a radioactive tracer was available for lutetium it was possible to do iTLC experiments instead of experiments with the spectrophotometer.

4.2. Labeling lutetium

4.2.1. iTLC

To determine the labeling efficiency of LuDOTA, iTLC was used. In Figure 4.2 a clear separation between free lutetium and LuDOTA can be seen. The experiments have been done in triplicate to be sure that a consistent separation is possible. iTLC silica gel strips were used for the stationary phase and 5% acetonitrile as the mobile phase, as described in the literature [25].

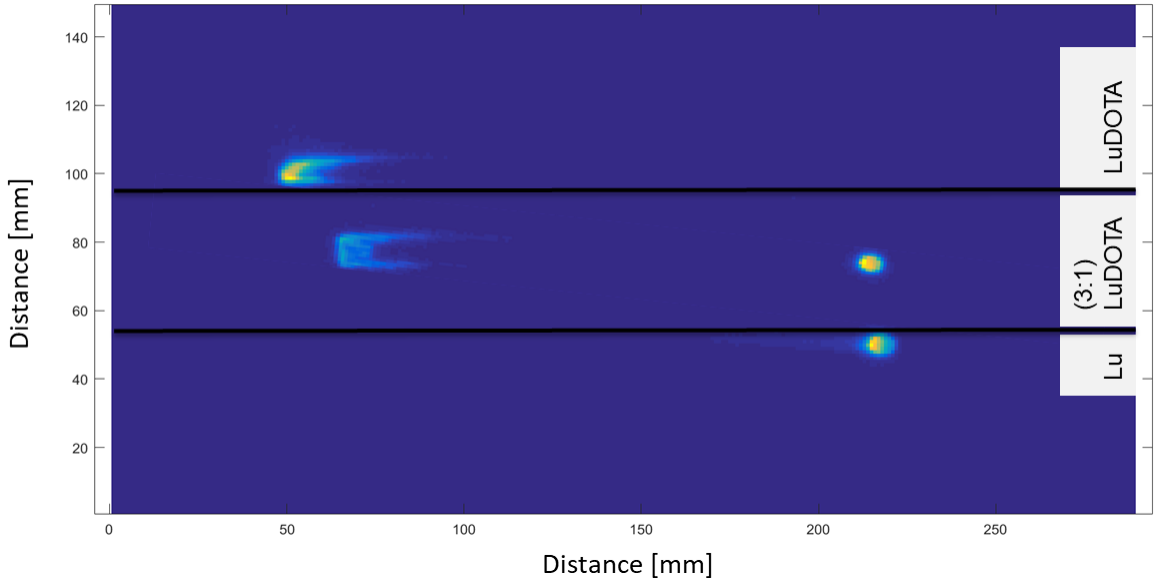

Figure 4.2: The visualisation of the separation of free lutetium and LuDOTA using iTLC.

As can be seen in Figure 4.2 LuDOTA goes up with the mobile phase and free lutetium stays at the origin, the sample in the middle shows the separation of a (3:1) LuDOTA sample, meaning 1/3 is LuDOTA and 2/3 is free Lu. By measuring the percentage of the activity that stayed at the origin (free Lu) and the percentage that went up with the mobile phase (LuDOTA), the labeling percentage can be determined.

More mobile phases and stationary phases were tested, to determine if a separation between free lutetium and the lutetium-chelator complex was possible. An overview of these experiments is given in Table 4.1, these mobile phase and stationary phase combinations did not give a separation between free Lu and the complex. The reference on which the separation method was based is also given.

Table 4.1: An overview of mobile phases and stationary phases that did not give a (reproducible) separation. iTLC/TLC means both stationary phases were tried.

Complex	Stationary Phase	Mobile Phase	Reference
LuEDTA	iTLC/TLC silica gel	saline solution (0.9% NaCl)	[49]
LuDTPA	iTLC/TLC silica gel	ammonium hydroxide : methanol : water (1:20:20)	[50]
LuDTPA	iTLC silica gel	saline	[63]
LuDOTA	iTLC/TLC silica gel	ammonium hydroxide : methanol : water (1:20:20)	[50]
LuDOTA	iTLC/TLC silica gel	10% ammonium acetate : methanol (1:1)	[64]
LuDOTA	iTLC/TLC silica gel	saline solution (0.9% NaCl)	[65]
LuDOTA	iTLC silica gel	EDTA-NH_4Ac	[66]

The separation of LuDTPA and Lu with ammonium hydroxide : methanol : water (1:20:20) and TLC strips was performed as was described in the literature [50]. The other separation were based on the literature, however, in the literature a different separation was done. Saline was chosen based on the iTLC separations of three researches: the separation of Lu and Lu–DOTA coupled to an antibody [49], the separation of Tc and Tc-DOTA coupled to a nanocolloid [65] and the separation of Tc and Tc-DTPA [63]. The mobile phase 10% ammonium acetate : methanol (1:1) was based on the separation of Lu-[bis-(phosphonomethyl))carbamoyl] methyl-7,10-bis(carboxymethyl)-1,4,7,10-tetraazacyclododec-1-yl)acetic acid (BPAMD) and Lu with iTLC as stationary phase [64]. The mobile phase EDTA-NH_4Ac with iTLC was based on the separation of ^{111}InDTPA [66]. That the combinations of mobile phases and stationary phases did not give a separation for Lu and LuDOTA, is probably because the methods were described for different complexes and especially for different chelators. However, for LuDTPA with ammonium hydroxide : methanol : water (1:20:20) and TLC the complex was the same, therefore, it is unclear why a reproducible separation was not possible. An explanation could be that the TLC strips were not treated exactly the same for each measurement. Because, for separation with iTLC, it is important that all strips are treated in the same way. Same size, same time in the development chamber, same mobile phase and the sample should not touch the mobile phase [59].

4.2.2. Temperature and ratio

The labeling efficiency was determined for different temperatures and ratios of lutetium with DOTA. The labeling was performed for the temperatures ranging from 20°C to 90°C. The results for 20°C and 30°C are given in Figure 4.3a. The results for 40°C - 90°C are given in Figure 4.3b.

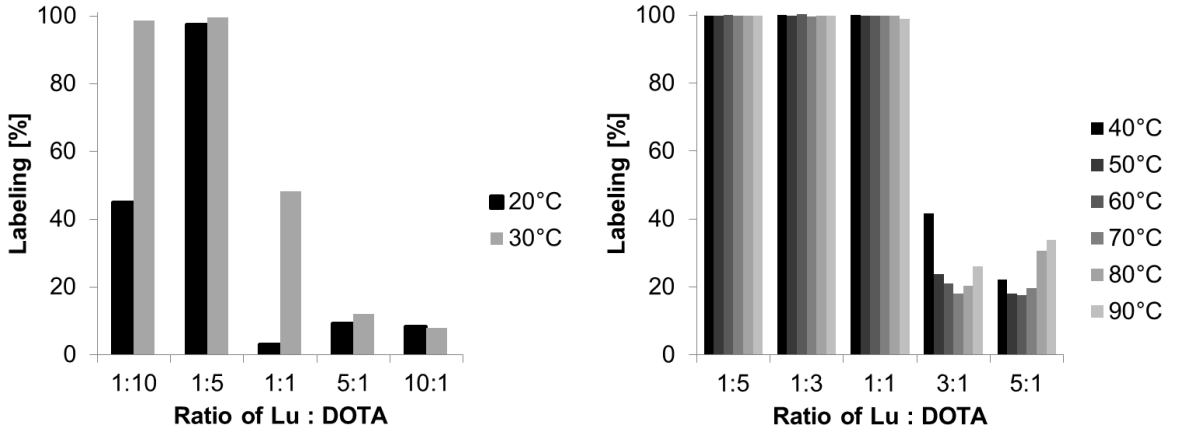

(a) The labeling percentage between lutetium and DOTA as a function of the ratio at 20°C and 30°C.

(b) The labeling percentage between lutetium and DOTA as a function of the ratio and the temperature range 40°C to 90°C, respectively from left to right.

Figure 4.3: The labeling percentage between lutetium and DOTA as a function of the ratio and the temperature.

From the Figures 4.3a and 4.3b it can be concluded that (1:1)LuDOTA labeling is possible, when labeling is done from 40°C up to 90°C. Smaller ratios were used for the higher labeling temperatures, because smaller ratios are preferred. The smaller ratios are preferred, because if a labeling of (1:1)LuDOTA is possible there is the least amount of necessary DOTA in the loop, resulting in less DOTA to with which the free lutetium can relabel. This means that labeling with a (1:1) ratio would be optimal. From literature it was found, that the labeling would be better at higher temperatures, since in literature a labeling temperature of 90°C is used [25, 49, 50, 64]. As can be seen in Figure 4.3b this is actually not necessary, depending on the ratio of Lu:DOTA, 100% labeling can already be achieved at 40°C.

The labeling in Figure 4.3a at Lu:DOTA ratios of (1:5) and (1:10) were unexpectedly low. A higher labeling percentage would be expected for labeling experiments containing an excess of DOTA, since this increases the number of labeling sites, and thus the chance for lutetium to bind to the chelator. This could indicate that the process is unstable at room temperature. At 30°C the result is as expected, a higher labeling percentage when a higher amount of DOTA is present. In Figure 4.3b the experimental results obtained for the (3:1) ratio at 40°C is deviating from the other results, this could be a coincidence since the experiment has been done only once. It has been chosen to do the experiments only once, since the goal was to see a trend in the

labeling. Furthermore, the amount of tracer can be neglected in determining the ratio, since in general the stock solution of ^{177}Lu was around 240 MBq in 20 μL, from which a dilution was made of approximately 20 kBq/μL. This results in a molarity in the order of 10^{-20} mol/L. This is negligible when using samples in the order of mmol/L. Based on the results above and the literature [25] it was determined to use the protocol of 15 minutes at 90°C and 300 rpm in the thermoshaker for labeling (1:1)LuDOTA.

4.2.3. Solvent

The labeling percentage for (1:1)LuDOTA as a function of the time at 40°C was determined. This was done to determine how fast relabeling will happen in the loop, since it will likely be 40°C inside the loop. The labeling was determined for three different solutions, in which the samples were prepared, being a pH 4.3 HCl solution, MQ and a 1 M sodium acetate acetic acid pH 4.3 buffer. The percentage of labeling was determined after 1, 3, 5, 10 and 15 minutes, see Figure 4.4.

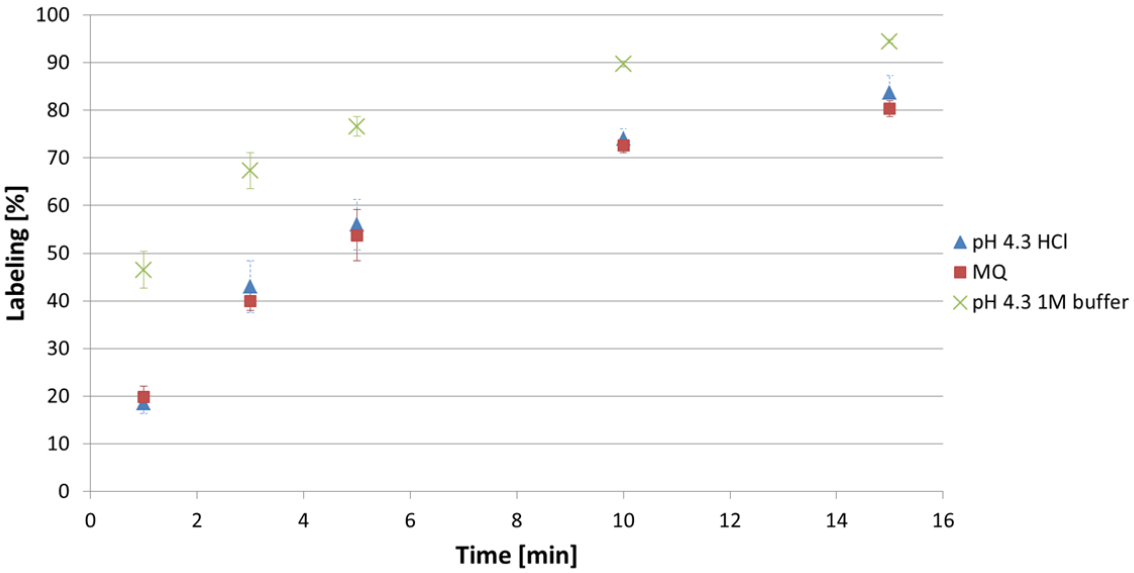

Figure 4.4: The percentage of labeling as a function of the time for different solutions.

A longer labeling time also gives an increase in labeling, the best environment for the labeling of LuDOTA is the 1 M sodium acetate acetic acid buffer pH 4.3. The labeling is also possible in a pH 4.3 HCl solution and even possible when the sample is prepared only in MQ. The high labeling affinity at 40°C in MQ was not expected based on the literature [25], since there it was expressed that the labeling is pH dependent. It is beneficial that labeling is possible in the pH 4.3 HCl solution and MQ. Because, if either of those solutions could be used, there is less material in the solution in the loop, which would result in less radioactive by-products. By-products from the sodium acetate acetic acid buffer can be ^{24}Na, with a half-life of 15 hours, a cross section of σ = 5.3*10^{-5} b and a resonance integral of I$_0$ = 3.1*10^{-5} b [47, 67]. Another by-product is ^{14}C, with a half-life of 5730 hours, a cross section of σ = 1.4*10^{-7} b and a resonance integral of I$_0$ = 2.02*10^{-7} b [47, 68]. These cross section are low compared to the cross sections of holmium and lutetium, meaning that the chance that these by-products are produced is low. However, if it is not necessary, it is best to produce as little by-products as possible, especially if the by-product has a long half-life.

The results clearly show that the labeling is possible, even when MQ is used, the small error bars indicate a stable process. In Figure 4.4 it can be seen that at one minute already 20% of the LuDOTA is labeled when dissolved in MQ or pH 4.3 HCl and around 45% of the LuDOTA is labeled when it is dissolved in the buffer. This indicates that the labeling happens fast and this has to be taken into account in the calculations of the achievable SA in the loop, since it leads to relabeling. Two values have been determined for $f_{\text{relabeling}}$, which can be used in the calculations. The first value is for extraction after one round. One round in the loop takes 23 seconds, however the extraction takes place earlier than this, since it is part of the loop. This indicates that when extraction is done after each round, the extraction happens within a few seconds after the breaking of the LuDOTA complex. Based on Figure 4.4 it is assumed that there will not be instantaneously

relabeling, so for extraction after 1 round, $f_{\text{relabeling}} = 0$, indicating no relabeling. For irradiation of > 100 rounds, it is estimated that around 80% has relabeled, meaning $f_{\text{relabeling}} = 0.8$. This is an estimation, because the experiment was not performed for this long, therefore, the largest value from the experiment has been taken. This is a rough estimate, also because the situation is not the same in the experiment as it will be in the loop. In the loop the solution will flow, whereas during the experiment the solution was kept in an Eppendorf vial.

4.3. Stability lutetium

4.3.1. Time and temperature

The effect of time and temperature on the stability of the LuDOTA complex was investigated. This was done to determine whether the complex is stable at room temperature (RT) and at 40°C, likely the temperature inside the loop. In Figure 4.5 the stability is given as a function of time [h] for RT and 40°C. The measurements were done after 0.5, 1, 2, 4, 24, 72, 168 and 504 hours.

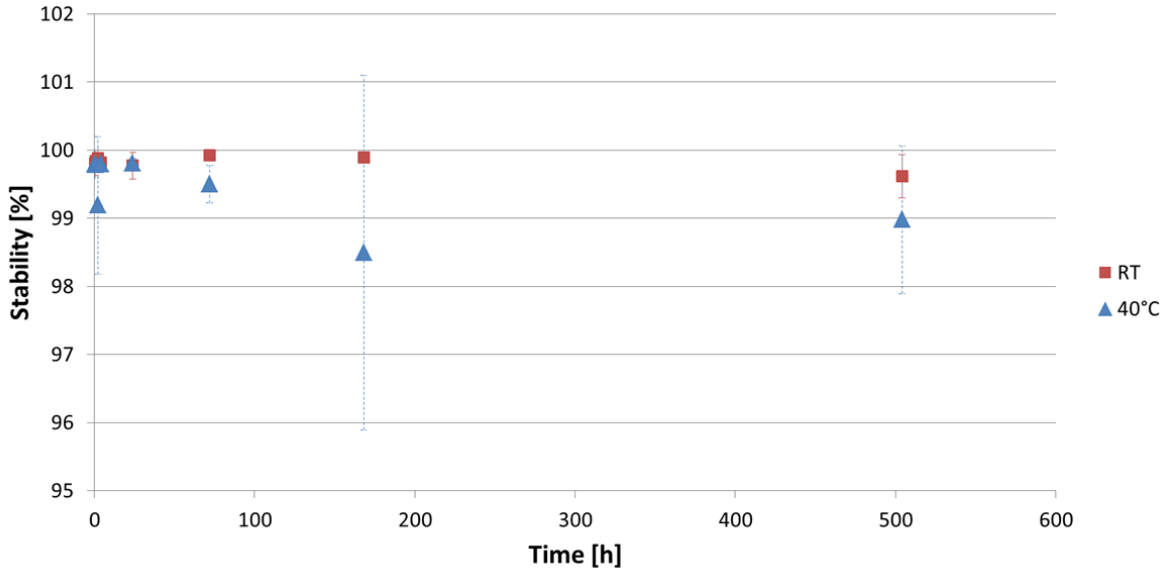

Figure 4.5: The stability measurement of LuDOTA at RT and 40°C.

Note that the y-axis goes from 95% to 102%, having a stability which is higher than 100% is not possible, however this interval on the y-axis has been chosen to have the full representation of the data, including the larger error bar that goes above 100%. Figure 4.5 shows that the complex is very stable both at RT as at 40°C for up to 504 hours (3 weeks). This was expected, based on the literature, because in the literature LuDOTA was measured to be a stable complex at 25°C and 37 °C [69]. The temperature of the samples during the measurements at 40°C was very stable since the whole sample was inside the thermoshaker. The RT was monitored during the experiment and was continuously at 20°C.

4.3.2. Gamma radiation iTLC

In Figure 4.6 the stability is given as a function of the dose [kGy]. The stability can be measured by measuring the ratio of complexed lutetium versus free lutetium. In Figure 4.6 it is shown that bond rupture between lutetium and DOTA has happened as a result of the gamma radiation. Because the samples were in the ^{60}Co source for 2 weeks, decay of the tracer has to be taken into account. Therefore, the ^{177}Lu that was added as the tracer, had an activity of 300 kBq, to enable the detection with the gamma detector after the 2 weeks.

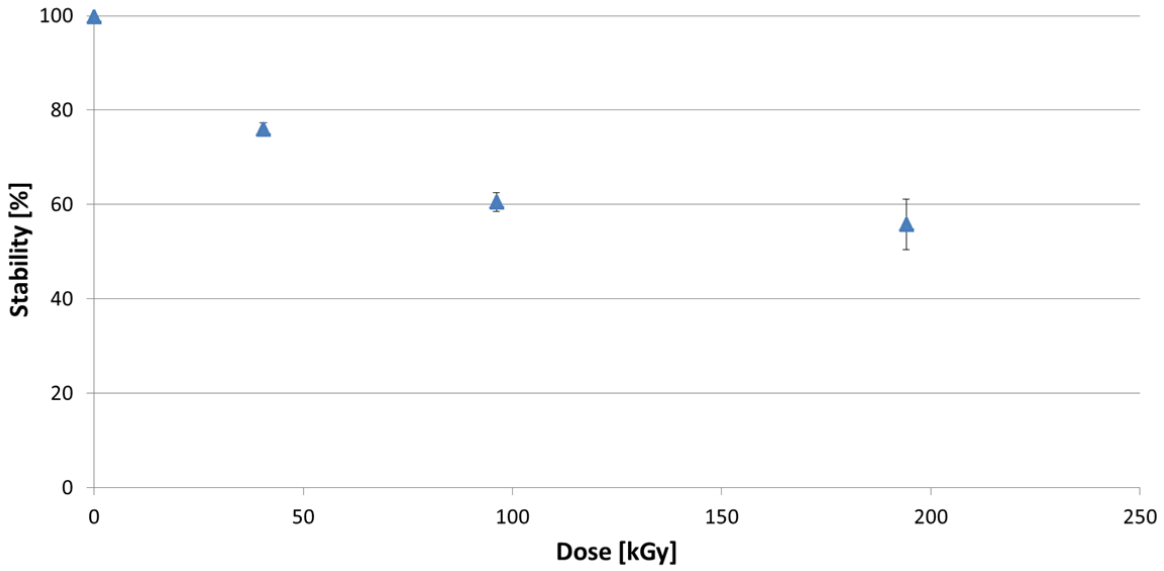

Figure 4.6: The effect of the gamma dose [kGy] on the stability of the LuDOTA sample.

The stability as a function of the dose, can be converted to the stability as a function of time in the DLDR tube or in the DLDR tube with the FlexBeFa shielding. The lead shielding from the FlexBeFa gives a different neutron flux and gamma dose rate. The shielding, as in the FlexBeFa, gives a factor 6.3 lower gamma dose rate, when assuming the same neutron flux [52]. The dose rate coming from the reactor core is 265 kGy/h [13], with the shielding this would result in a dose rate of 42 kGy/h. Based on this, the effect of the dose in the ^{60}Co source can be converted to a time in the DLDR tube, with or without shielding. A best fit has been made, by interpolating the data points, for the stability as a function of time. This was done for the DLDR tube, both with and without shielding. The fits can be used in the calculation of the radiolysis. The best fits for the DLDR tube and the DLDR tube with FlexBeFa shielding are given in equation 4.1.

$$\begin{aligned} f &= -3.246 * t^{0.3397} + 101.3 \\ f_{\text{FlexBeFa}} &= -1.584 * t^{0.3474} + 100.6 \end{aligned} \tag{4.1}$$

The f gives a percentage and t [h] is the time. A figure of the fit with the data points is given in Figure A.1 for the DLDR tube and in Figure A.2 in appendix A. It must be noted that the fitted equations are such that at t=0 the fit does not correspond to 100% stability. The fitted functions give f = 101.3% and f=100.6%, respectively, for t=0, which is not possible. Since one of the experimental data points corresponds with stability = 100% at t=0, this shows that the fitted functions have an uncertainty. However, the fitted function were still used to determine the corresponding equations to calculate the fraction of radiolysis, $f_{\text{radiolysis}}$. These are given in equation 4.2.

$$\begin{aligned} f_{\text{radiolysis}} &= (100 - (-3.246 * t^{0.3397} + 101.3))/100 \\ f_{\text{radiolysisFlexBeFa}} &= (100 - (-1.584 * t^{0.3474} + 100.6))/100 \end{aligned} \tag{4.2}$$

The $f_{\text{radiolysis}}$ is the fraction of radiolysis. For t=0 the fraction of radiolysis should be 0, because this corresponds with the measurement of 100% stability at t=0. However, because of the uncertainty in both of the fitted functions, the fraction of radiolysis becomes negative for small values of t. The function for $f_{\text{radiolysis}}$ gives negative values for the first 244 seconds. The function for $f_{\text{radiolysisFlexBeFa}}$ gives negative values for the first 221 seconds. This corresponds to approximately 4 minutes, on a time-scale of hours. Because the fraction of radiolysis has to be zero at t=0, there are two options of adapting the fitted functions, which is necessary since negative numbers are not possible. The first option is to force the $f_{\text{radiolysis}}$ to start at 0 for t=0, this is done by a shift over the y-axis, by changing 101.3 and 100.6, respectively, to 100. In Figure 4.7 the fraction of radiolysis is given when this forced start at 0 is applied. A magnification of the lines for the first minutes is

also given. The new equations are given by equation 4.3. The other option is to assign $f_{\text{radiolysis}}$=0 when the value is negative. This is shown in Figure 4.8 and the equations are given in equation 4.4.

$$\begin{aligned} fs_{\text{radiolysis}} &= (100 - (-3.246 * t^{0.3397} + 100.0))/100 \\ fs_{\text{radiolysisFlexBeFa}} &= (100 - (-1.584 * t^{0.3474} + 100.0))/100 \end{aligned} \tag{4.3}$$

$$\begin{aligned} fc_{\text{radiolysis}} &= (100 - (-3.246 * t^{0.3397} + 101.3))/100 \\ \text{if } f_{\text{radiolysis}} < 0 &: fc_{\text{radiolysis}} = 0 \\ fc_{\text{radiolysisFlexBeFa}} &= (100 - (-1.584 * t^{0.3474} + 100.6))/100 \\ \text{if } fc_{\text{radiolysisFlexBeFa}} < 0 &: fc_{\text{radiolysisFlexBeFa}} = 0 \end{aligned} \tag{4.4}$$

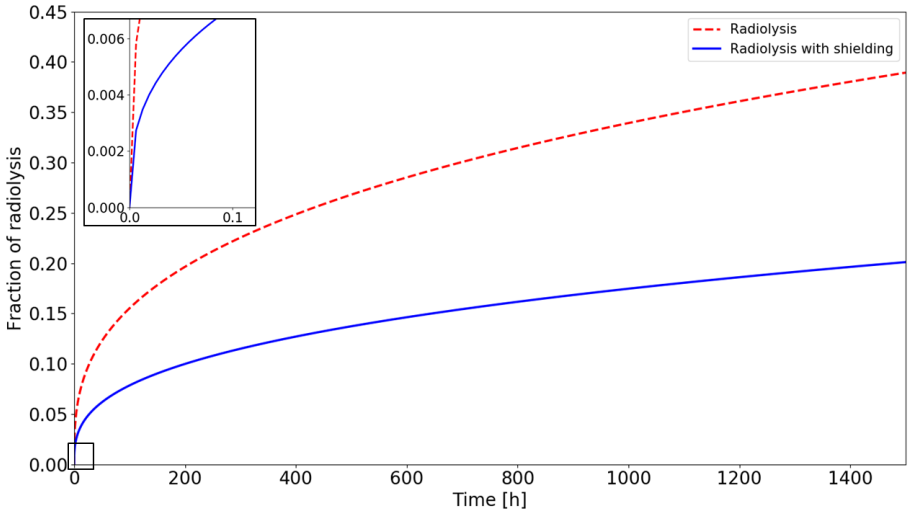

Figure 4.7: The fraction of radiolysis for the fits that has been shifted over the y-axis, $fs_{\text{radiolysis}}$ and $fs_{\text{radiolysisFlexBeFa}}$.

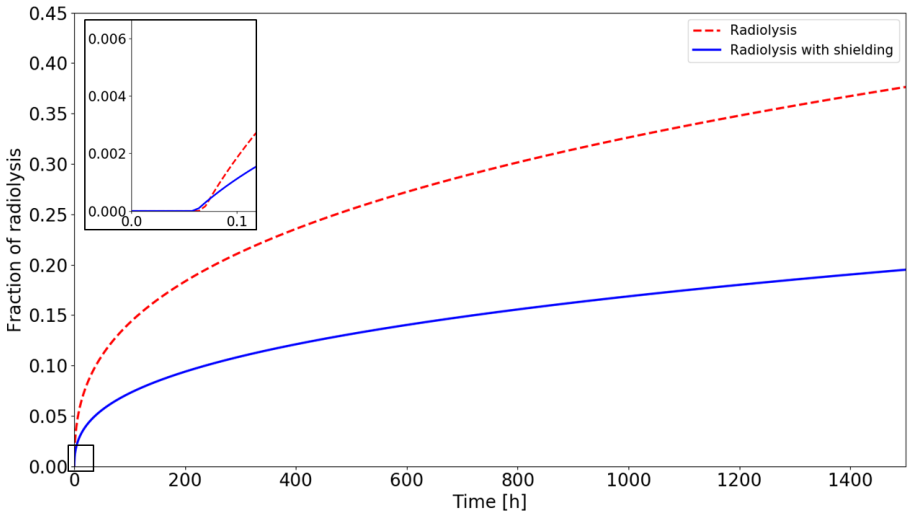

Figure 4.8: The fraction of radiolysis for the fits that has been cut-off, this means the negative values are assigned to be zero, $fc_{\text{radiolysis}}$ $fc_{\text{radiolysisFlexBeFa}}$.

Since the shielding of the FlexBeFa corresponds to a lower dose rate, the fraction of radiolysis, at a certain time, is expected to be lower than without the shielding. This corresponds with the results in Figures 4.7 and 4.8. In general there is a decrease in stability as a result of the gamma dose from the ^{60}Co source. This decrease in stability was expected, because this has also been reported in the literature [14]. Furthermore, the reference samples, which were under the same conditions except for the gamma radiation, did not show a decrease in stability, therefore, this decrease is indeed due to the gamma radiation.

A fit for the stability as a function of time is given for both the DLDR tube and the DLDR tube with FlexBeFa shielding. This was done to give an indication of the stability under gamma radiation. The gamma radiation in the ^{60}Co source is not the same as in the DLDR tube, which is close to the reactor core. The energy of the gamma radiation is different in the two situations [30]. Furthermore, the fitted functions, with and without shielding, have a large uncertainty for short irradiation times (approximately 4 minutes). This is because for short irradiation time, the function has either been shifted or cut-off, to prevent negative values. Probably, neither of the fitted functions gives the correct situation, since for example, having no radiolysis is unlikely. However, given the data that is available, these fits were made as closest available approximations, to be able to determine the effect of radiolysis. Because of the uncertainty for short irradiation time, both options for the fitted functions will be tested in the model, meaning $fs_{\text{radiolysis}}$ and $fc_{\text{radiolysis}}$ will be used to simulate the radiolysis fraction in the DLDR tube and $fs_{\text{radiolysisFlexBeFa}}$ and $fc_{\text{radiolysisFlexBeFa}}$ will be used for the simulation in the DLDR tube with shielding.

4.3.3. Gamma radiation NMR

The effect of the gamma radiation on the structure of the sample was measured with NMR. This measurement was done for samples without a radioactive tracer. These samples were measured to determine if bond rupture in the DOTA complex would happen, because of the gamma radiation. Furthermore, the reference sample, DOTA dissolved in D_2O and the sodium acetate acetic acid buffer have been measured. The NMR spectra are given in figure 4.9.

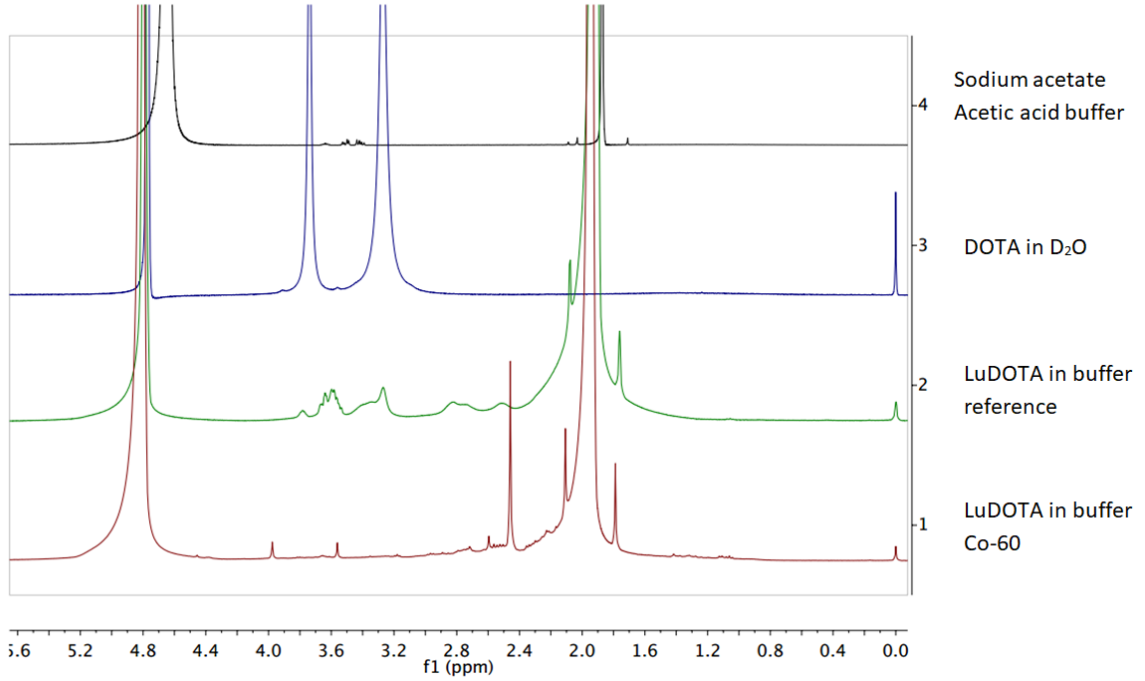

Figure 4.9: The results of the NMR measurements for the buffer, DOTA, LuDOTA as a reference and LuDOTA having been irradiated in a ^{60}Co source with 298.5 kGy.

The peaks of the sodium acetate acetic acid buffer are slightly shifted compared to the peaks of the other samples. This can be, because the measurement was not done on the same day. However it can be concluded that the peaks correspond to the same H-atoms as in the other samples, since the peaks are given in regions, corresponding to certain bonds [70]. The peak at 0 ppm belongs to the TMS [70, 71], this peak is missing for the sodium acetate acetic acid buffer, since D_2OTMS was not added to this sample. This made the calibration also more difficult. The broad peak around 2 ppm belongs to the sodium acetate acetic acid buffer. The peak of sodium acetate is at 1.92 ppm [72] and the peak of acetic acid at 2.09 ppm [73]. This can be checked since the buffer was not present in the DOTA sample and in that sample the peak is not visible. The peaks between 3.0 ppm and 4.0 correspond to DOTA [74, 75] and 4.8 ppm corresponds to D_2O [75].

When looking at the sample that has been irradiated in the ^{60}Co source, the 'LuDOTA in buffer Co-60' sample, in Figure 4.9, the peaks at 3.6 ppm and 4.0 ppm are the peaks corresponding to DOTA, indicating that some LuDOTA bonds have been broken. This was also confirmed by the results in Figure 4.6. The peak at 2.4 ppm could indicate that the gamma radiation affected the buffer, resulting in a disconnected CH_3 part of the buffer [70]. This disconnected part cannot correspond to DOTA, since the intensity of the peak at 2.4 ppm is higher than the intensity of the peaks corresponding to DOTA, meaning there is not enough DOTA present to have this many disconnected parts. At 3.2 ppm and 4.4 ppm there are small peaks, which are not present in the LuDOTA reference sample, these could indicate broken CH_2 parts of DOTA or these peaks indicate noise. The peaks are difficult to see and therefore an enlarged image can be found in Figure 4.10, with the arrows indicating the peaks. In general based on these results, if the structure of DOTA is affected by the gamma radiation, then only a small fraction of the DOTA is affected, which indicates that DOTA seems to be stable under the gamma radiation.

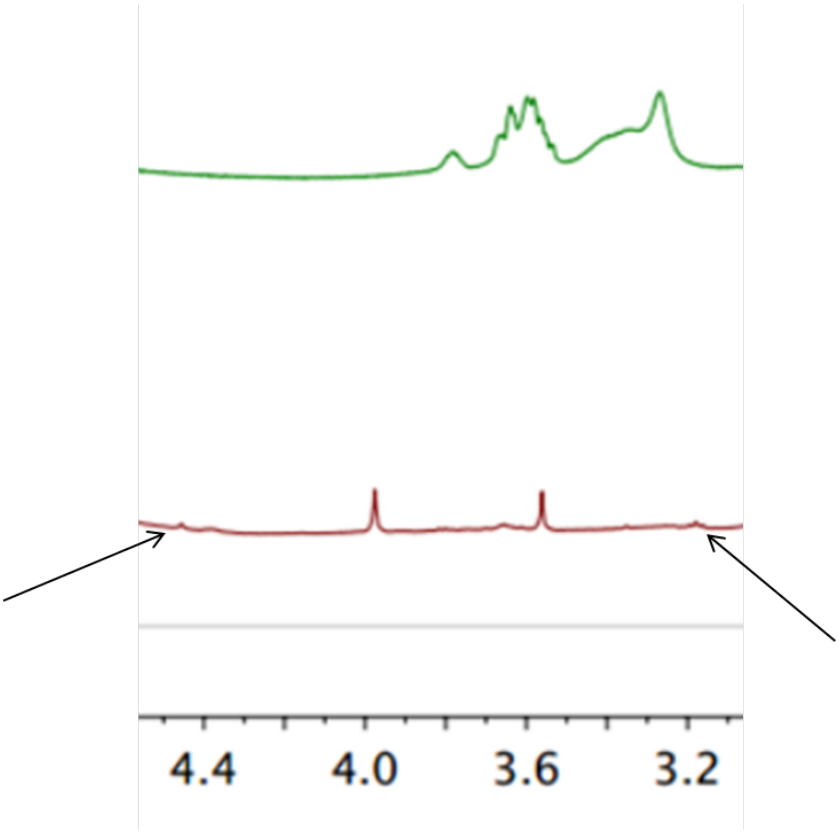

Figure 4.10: The zoomed in part of the NMR spectrum of the LuDOTA sample from the ^{60}Co source and the reference sample.

4.4. Extraction lutetium

To see if separation between free lutetium and LuDOTA is possible, a proof of concept for ion-exchange was done. For this proof of concept the binding of the free lutetium and LuDOTA with the resins was determined. The binding with the resins depends on the acidity of the wash. The binding is expressed as the percentage of the activity that binds to the resin and is plotted as a function of the molarity of HCl, in Figure 4.11.

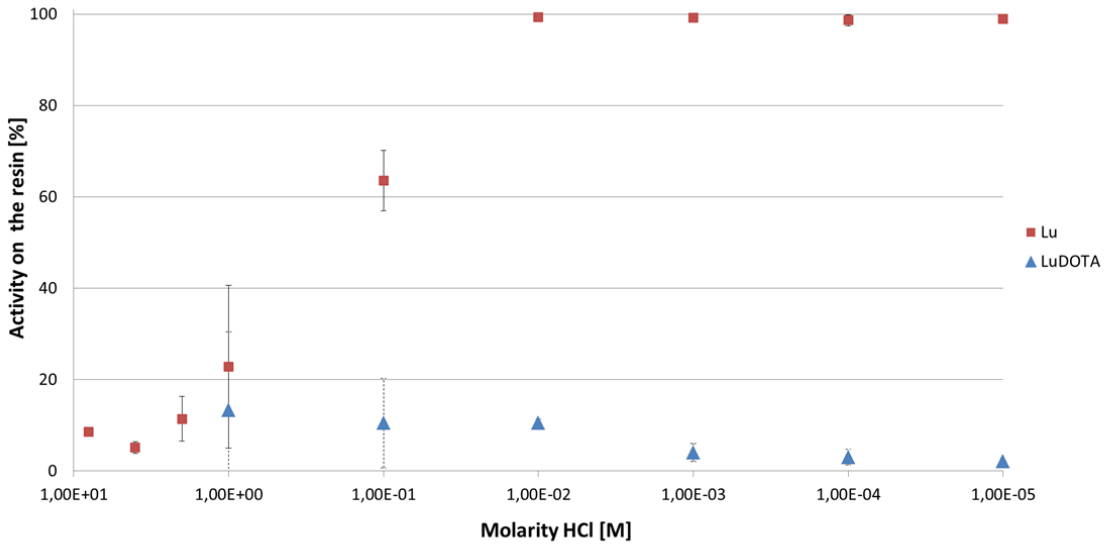

Figure 4.11: The percentage of the activity attached to the resin, showing the binding with resins of LuDOTA and free Lu depending on the amount of HCl in the wash. Going from a higher molarity to a lower molarity of HCl.

Figure 4.11 shows that for a more acidic environment the binding of lutetium with the resins is lower. This is in line with the literature [55]. LuDOTA barely shows any binding with the resins, meaning it remains in the liquid phase. This is because, LuDOTA is an anion and the used resins are cation exchange resins [53, 54]. For 10^{-5} M HCl (pH 5) 100% lutetium and almost 0% LuDOTA remains on the resins. Hence, washing with a 10^{-5} M HCl solution results in a complete separation between lutetium and LuDOTA. The lutetium remains on the resins, whereas the LuDOTA remains in the liquid phase. After this the resins can be washed with a higher molarity HCl solution, to wash the lutetium of the resins, into another liquid phase. This solution contains only the activated lutetium, which can be used for treatment. According to Figure 4.11, 4 M HCl can be used for eluting the lutetium from the resins, because lutetium shows the lowest affinity with the resins at 4 M HCl. The experiments for LuDOTA with a wash of more than 1 M HCl have not been performed since the current graph, in Figure 4.11, already gives all the information needed.

To verify whether a separation is indeed possible, an extraction experiment has been done. For this experiment a sample was used with 40% LuDOTA and 60% free lutetium, as was determined with iTLC. After the first wash, approximately 60% of the activity (i.e. the free ^{177}Lu) should remain on the resin. After the second wash almost 0% of the activity should remain on the resin, since the free lutetium should be eluted. The first wash was performed with a 10^{-5} M HCl solution. The second wash was done with a 4 M HCl solution, the results of this extraction are given in Figure 4.12.

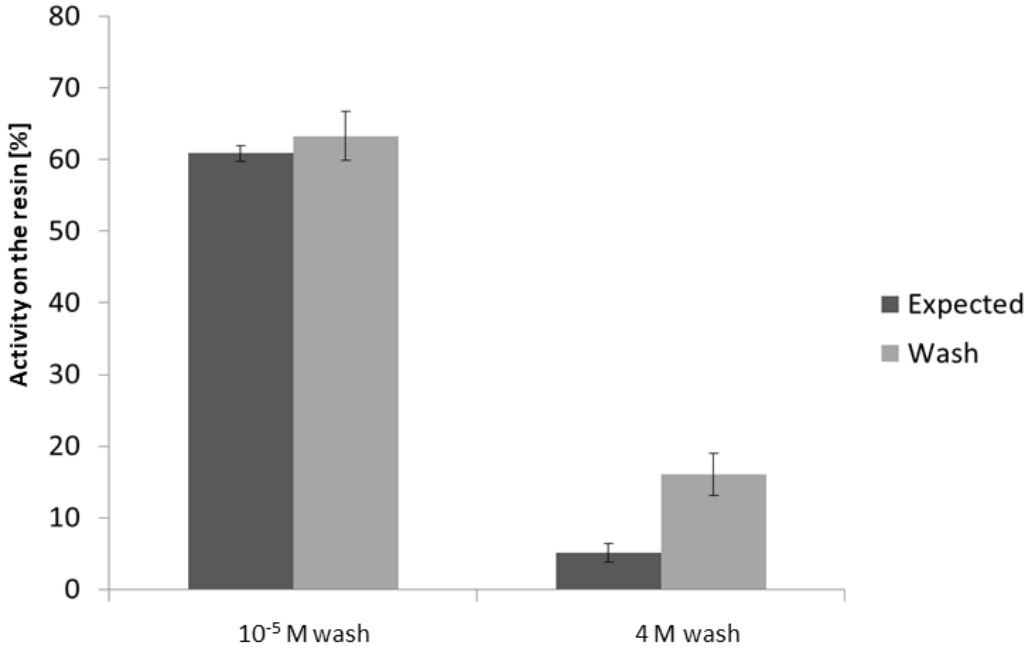

Figure 4.12: The activity on the resin, the expected result and the actual result after washing. To determine the fraction of free lutetium that was extracted.

Figure 4.12 shows the expected and the actual result. The result after the wash with the 10^{-5} M HCl solution is inside the expected range. The second wash shows that more activity remained on the resins than was expected, so less free lutetium was eluted. Based on the results in Figure 4.11, only a few percent of the lutetium should be retained on the resins. This makes it unclear why there is more lutetium on the resins than was expected. It could be that the liquid phase was not homogeneous.

However, in general the results show that a separation between lutetium and LuDOTA is possible using these resins. In the current setup it results in the extraction of 84% of the lutetium. This can be used in the calculation for the specific activity as $f_{\text{extraction}} = 0.84$.

For the extraction experiments that were done, it was assumed that the liquid phase is homogeneous, so it can be assumed that the liquid that remained in the Eppendorf vial with the resins contains the same concentration of Lu and LuDOTA. This is needed to calculate the actual activity on the resins and in the liquid phase. The experiments have been done using Eppendorf vials, the extraction has not been done using a column. Therefore, these experiments were proof of concept experiments. The proof of concept experiments show that separation of free Lu and LuDOTA using ion exchange columns is feasible. The exchange with the resins will probably be different when are used, since there is more reaction surface but less reaction time. Therefore, the velocity of the solution and the length of the column have to be optimized.

The measurements of the very acidic samples ($\geq$ 1 M HCl) were done with a germanium detector. Since only the measurements of the two Eppendorf vials that originated from the same sample are quantitatively compared, those measurements always have to be done with the same detector. For the different samples it is not of importance if they are measured with the same detector since only percentages are compared.

4.5. Theoretical specific activity

The above results for relabeling, radiolysis and extraction, in combination with the constant for F from Zhernosekov et al. [14] have been used to determine the theoretically possible specific activity. The specific activity has been calculated for both holmium and lutetium in the DLDR tube and for the DLDR with the lead shielding from the FlexBeFa. The shielding from the FlexBeFa results in a factor 6.3 lower gamma dose rate, when assuming the same neutron flux.

For all the calculations the following parameters have been the same: $V = 0.5$ L, $v = 0.025$ m/s, $M = 10$ mmol/L, $F = 0.132$, $f_{\text{extraction}} = 0.84$. For extraction after 1 round, $f_{\text{relabeling}} = 1$ and for extraction after > 100 rounds, $f_{\text{relabeling}} = 0.2$. For both the holmium and lutetium complex it has been experimentally tested that 10 mmol/L can be dissolved in MQ. For $f_{\text{radiolysis}}$ the fitted functions from equations 4.3 and 4.4 have been used.

4.5.1. Holmium

For holmium an irradiation time of $t_{\text{irr}} = 240$ hours has been used. The input material is ^{165}HoDOTA. The natural abundance of ^{165}Ho $h = 1$ with the molar mass $M = 164.93$ g/mol. The half-life of ^{166}Ho is $t_{\frac{1}{2}} = 26.4$ h [30]. The thermal cross section is $\sigma = 58 * 10^{-24}$ cm^2 and the resonance integral is $I_0 = 632 * 10^{-24}$ cm^2 [47]. For these experiments it has been used that extraction of ^{166}Er is possible [76], this is the decay product of ^{166}Ho. In Figure 4.13 the activity [GBq], when taking into account the Szilard-Chalmers effect, is shown.

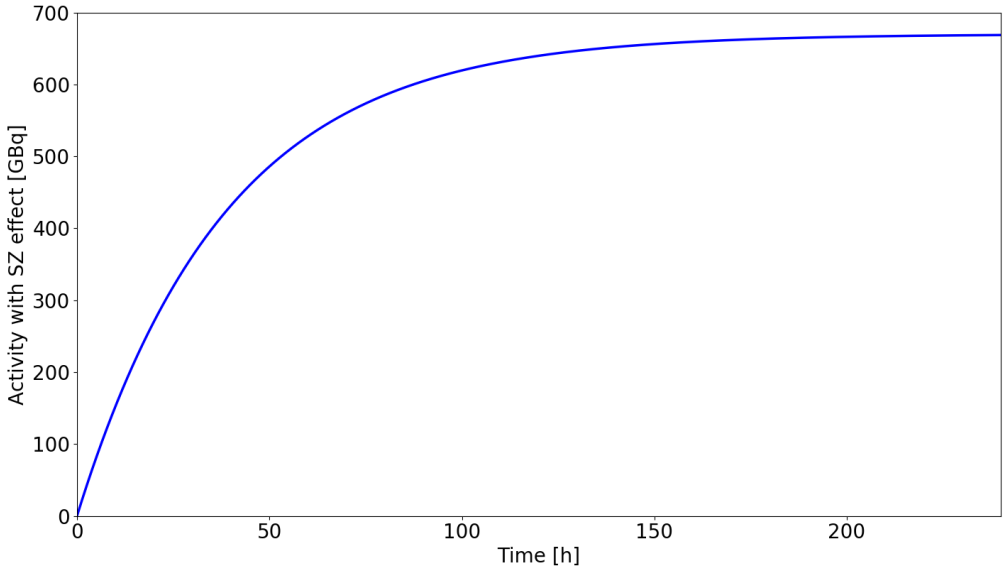

Figure 4.13: The activity as a function of the irradiation time when taking into account the Szilard-Chalmers effect, the maximum activity is A = 636 GBq.

The maximum activity is A = 636 GBq. The activity stabilizes to this value because of the equilibrium that is reached between decay and activation [26]. The results for the specific activity, when using the properties of the loop are given. In Figure 4.14 the result is given, when the shifted equations for $f_{\text{radiolysis}}$, are used. These equations were given in equation 4.3.

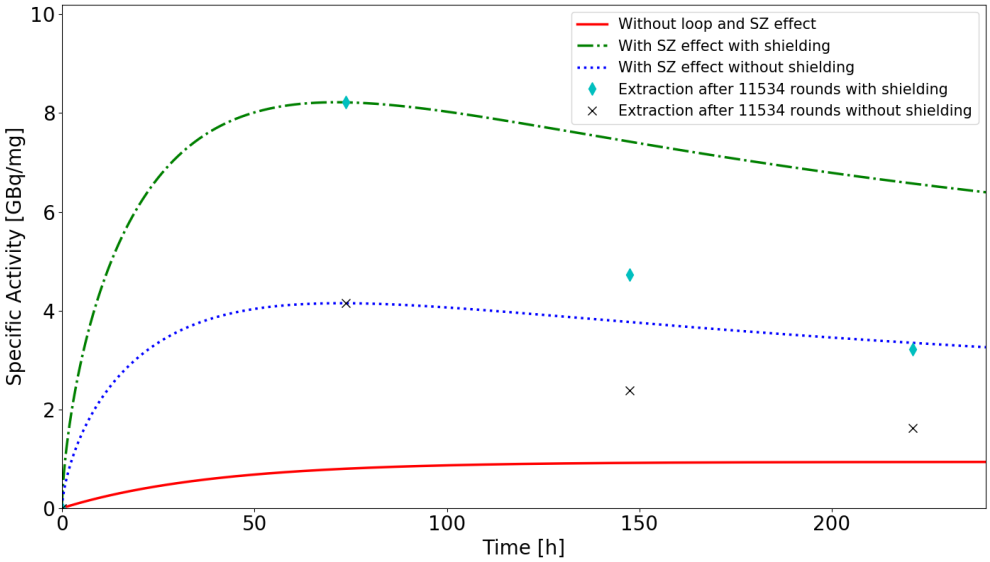

Figure 4.14: The specific activity as a function of the time. Given for the calculation with the loop and SZ effect, with only the SZ effect and with the SZ effect and the loop properties. The shifted radiolysis fit was used.

The red line gives the SA without the SZ effect and the loop system. The green dash-dot line and the blue dotted line give the SA when using the SZ effect without in between extraction, for with and without shielding, respectively. The in between extraction is indicated by the cyan diamond and the black x, for with and without shielding, respectively. These data points give the specific activity of the 'bulk'. The bulk contains all the batches that have been extracted up to that point. The in between extraction in the loop is, each time, done at the maximum possible specific activity. This maximum is only reached after a certain amount of time, because the amount of radiolysed target material is dominant over the amount of recoiled radionuclides. Therefore, new recoiled radionuclides increase the activity, however their mass is negligible. This results in an increase of specific activity. The SA starts to decrease again, due to an increase of radiolysis.

In this situation it is more beneficial to use the SZ effect and extract after the total irradiation time, than having in between extraction. This is because, if a batch is extracted it is collected in the 'bulk' (on the column), this batch that is extracted contains both ^{165}Ho and ^{166}Ho. The ^{166}Ho in the 'bulk' decays, which lowers the activity. The mass in the 'bulk' also decreases, because the decay product, ^{166}Er, does not have to be taken into account because separation is possible. However, the ^{165}Ho remains in the 'bulk'. If a new batch is added, which has again the maximum possible specific activity, the total specific activity becomes lower. This is because the new specific activity in the 'bulk' is a combination of the specific activity that was already in the 'bulk' and the specific activity of the new batch. Since the specific activity in the 'bulk' was lower due to decay, the total new specific activity is lower than the maximum SA.

The result when using the cut-off equations, equation 4.4, is given in Figure 4.15. The result is only given for a short irradiation time, to give an overview of the process. The result for the irradiation time of t=240 hours is given in Figure A.3 in appendix A. The red line for 'Without loop and SZ effect' is the same as in Figure 4.14, it only appears to be zero because of the scale of the y-axis.

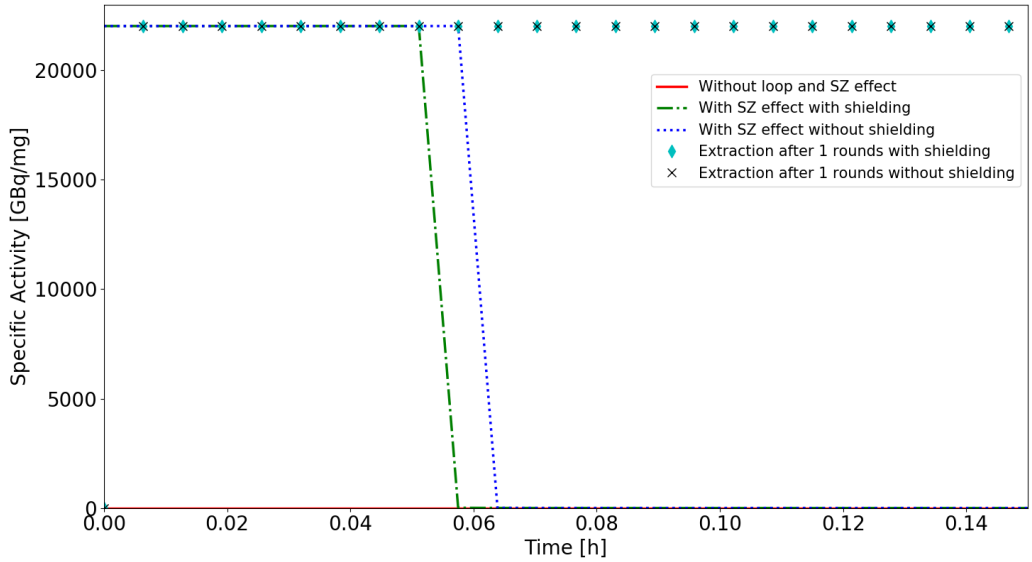

Figure 4.15: The specific activity as a function of the time, only given for a short radiation time. Given for the calculation with the loop and SZ effect, with only the SZ effect and with the SZ effect and the loop properties. The cut-off radiolysis fit was used.

Since the $f_{\text{radiolysis}} = 0$ for short irradiation time, the maximum specific activity is immediately reached. If extraction is done after each round, a batch with this maximum specific activity is added to the 'bulk' (the column) each round. The ^{166}Ho collected in the 'bulk' will decay, however the mass of the decay product does not have to be taken into account, because separation of ^{166}Er is possible. This results in a constant specific activity in the 'bulk'. The fast decrease of specific activity, for the green dashed dotted line and the blue dotted line that correspond to not having in between extraction, correspond to the point where $f_{\text{radiolysis}}$ is not 0 anymore. This shows the large influence of the radiolysis on the achievable specific activity. The line that corresponds to 'without shielding' starts to decrease later than the line that corresponds to 'with shielding' this is because, the fitted function that corresponds to 'without shielding' gives negative values up to t=244 seconds, whereas the fit for 'with shielding' gives negative values up to t=221 seconds. This also shows the large uncertainty in the fitted functions, because the radiolysis should be less when shielding is applied and now the effect is less when there is no shielding.

An overview of the possible specific activities when making use of the Szilard Chalmers effect is given in Table 4.2. The SA is given for when the properties of the loop are used, with the corresponding parameters of the loop and also for the Szilard-Chalmers effect without the loop properties.

Table 4.2: The calculated SA [GBq/mg] at t=240 hours, when using the SZ-affect and with SZ effect in the loop. Depending on the parameters R_e, $f_{\text{radiolysis}}$, $f_{\text{extraction}}$, $f_{\text{relabeling}}$.

R_e	Shielding	$f_{\text{radiolysis}}$	$f_{\text{extraction}}$	$f_{\text{relabeling}}$	Calculated SA(t=240h) [GBq/mg] with loop	Calculated SA(t=240h) [GBq/mg]
11534	No shielding	shifted	0.84	0.8	1.62	3.26
11534	FlexBeFa	shifted	0.84	0.8	3.21	6.40
1	No shielding	cut_{off}	0.84	0	22015.01	3.48
1	FlexBeFa	cut_{off}	0.84	0	22015.01	6.79

For comparison the $SA_{\text{withoutSZ}} = 0.93$ GBq/mg. This means that when the shifted $fs_{\text{radiolysisS}}$ function is used, with the loop an increase of SA is achieved of a factor 3.45 and without the loop a factor of 6.88. When the cut-off radiolysis function $fc_{\text{radiolysisC}}$ is used an increase of SA, with the loop of a factor of 23672 is achieved and when only using the SZ effect the increase is a factor 7.3.

These values are an indication of what is possible when using the SZ-affect in the production loop. It must be noted that the radiolysis for short irradiation times has a large impact on the achievable specific activity. When there is no radiolysis, this gives an extreme value. If it is indeed possible to approach this extreme value, ^{166}Ho can be produced with a SA of a factor 2000x larger than the currently produced specific activities of 9.25–11.10 GBq/mg [77]. Furthermore, there will also be by-products created, such as ^{166m}Ho, which is a problem because of its half-life of 1200 years. Since its cross-section and resonance integral are lower than for ^{166}Ho ($\sigma = 3.1 * 10^{-24}$ cm^2 and $I_0 = 1.3 * 10^{-24}$ cm^2, respectively) this will only account for a small fraction of the total produced activity. Besides, the production of ^{166m}Ho is also a problem with the current production routes [23, 78]. Furthermore, for the calculations, the experimental results from this thesis of LuDOTA have been used. It is assumed that HoDOTA will react in a similar way as lutetium, since lutetium and holmium are both lanthanides. The lanthanides are a group which have very similar chemical properties [4], which makes it a valid assumption.

For confirmation of the code, extreme values have been calculated and compared with literature [26]. These extreme values are given in Table 4.3.

Table 4.3: The maximum possible SA [GBq/mg], calculated, calculated with the loop properties, theoretical. Depending on the parameters R_e, $f_{radiolysis}$, $f_{extraction}$, $f_{relabeling}$.

R_e	$f_{radiolysis}$	$f_{extraction}$	$f_{relabeling}$	Calculated maximum SA with SZ [GBq/mg]	Calculated maximum SA in loop [GBq/mg]	Theoretical SA [GBq/mg]
1	0	1	0	26208.35	26208.35	26863.47
1	0	0.84	0	22015.01	22015.01	22565.31

These values show that the maximum calculated SA is not higher than the maximum theoretical SA. Furthermore, the development of the mass was checked. The red dotted line gives the total mass of the target material and the blue line the mass of the uncomplexed nuclides, this line should never cross the red dotted line.

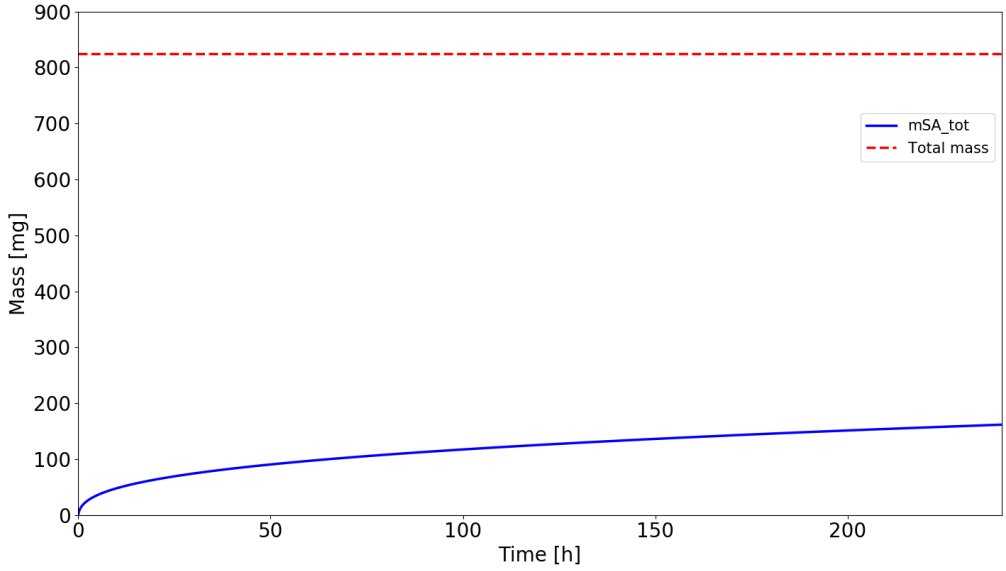

Figure 4.16: The total mass of the target material and the mass of the uncomplexed nuclides.

The mass of the uncomplexed nuclides does not become higher than the total mass of the target material and the maximum specific activity does not become higher than the theoretical maximum specific activity. Therefore, both checks confirm the correct functioning of the code.

4.5.2. Lutetium

For the lutetium simulations, an irradiation time of t_{irr} = 1500 hours has been used. The input material is LuDOTA. The natural abundance of ^{176}Lu is h = 0.0259, the molar mass M = 174.94 g/mol. The half-life of ^{177}Lu is $t_{\frac{1}{2}}$ = 6.64 days [30]. The cross section is $\sigma = 2020 * 10^{-24}$ cm^2 and the resonance integral is $I_0 = 1000 * 10^{-24}$ cm^2 [47]. For these experiments it has been used that extraction of ^{177}Hf is possible [79], this is the decay product of ^{177}Lu. In Figure 4.17 the possible activity [GBq] when taking into account the Szilard-Chalmers effect is shown.

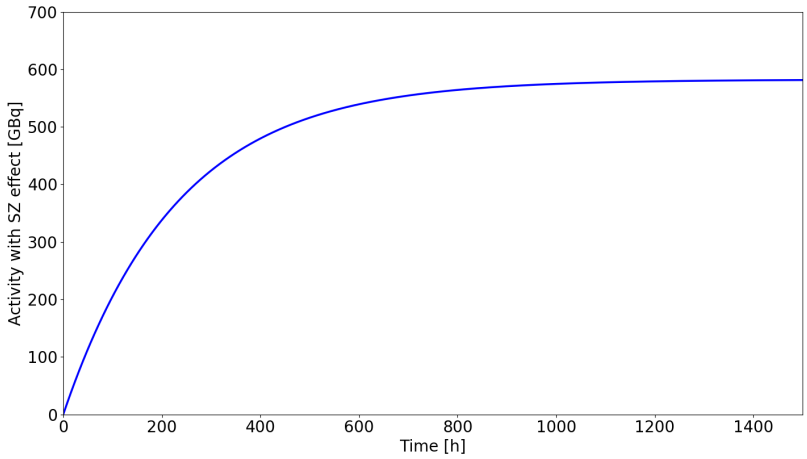

Figure 4.17: The activity as a function of the irradiation time when taking into account the Szilard-Chalmers effect, the maximum activity is A = 553 GBq.

The maximum activity is A = 553 GBq. Here the activity also reaches a maximum over time, due to decay. Also for lutetium the two different fits for $f_{\text{radiolysis}}$ have been investigated. In Figure 4.18 the result is given, when using the shifted equations for $f_{\text{radiolysis}}$, as given in equation 4.3.

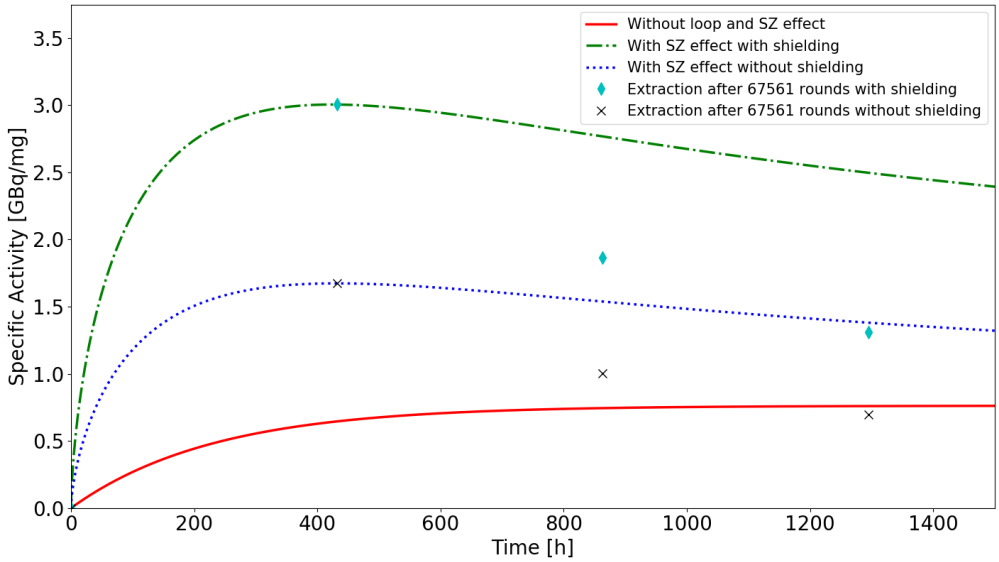

Figure 4.18: The specific activity as a function of the time. Given for the calculation with the loop and SZ effect, with only the SZ effect and with the SZ effect and the loop properties. The shifted radiolysis fit was used.

The red line gives the SA without the SZ effect and the loop system. The green dash-dot line and the blue dotted line give again the SA when using the SZ effect without in between extraction. The in between extraction is indicated by the cyan diamond and the black x. This extraction was done for batches with the maximum specific activity. Also for lutetium the maximum is reached after a certain time, because of the dominance of the amount of radiolysed target material in the beginning. As a result of this, the mass that corresponds to the increase of activity, is negligible. This results in an increase of specific activity. The SA starts to decrease again, due to an increase of radiolysis.

Also for lutetium it is more beneficial to use the SZ effect and extract after the total irradiation time, than having in between extraction. This is because if a batch is extracted it remains in the 'bulk' (on the column), this batch that is extracted contains both ^{175}Lu/^{176}Lu and ^{177}Lu. The ^{177}Lu in the 'bulk' decays, which lowers the activity in the 'bulk'. The mass of the decay product, ^{177}Hf, does not have to be taken into account since separation is possible. However, the ^{175}Lu/^{176}Lu remain in the 'bulk'. If a new batch is added to the 'bulk', which has again the maximum possible specific activity, the total specific activity is lower, because the specific activity in the 'bulk' was lower due to decay.

The result when using the cut-off equations, equation 4.4, is given in Figure 4.19. The result is only given for a short irradiation time, to give an insight in the process. The result for the irradiation time of t=1500 hours is given in Figure A.5 in appendix A.

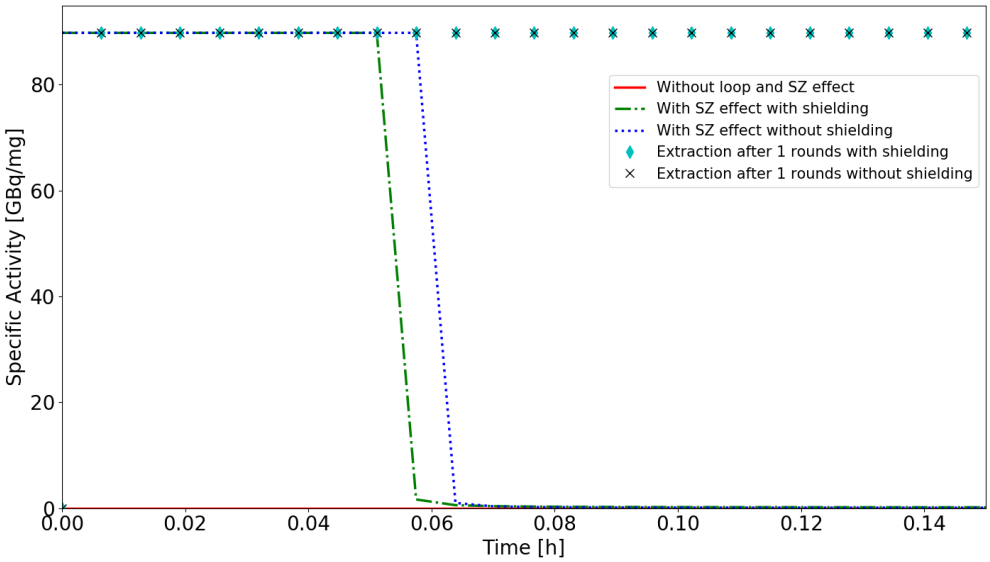

Figure 4.19: The specific activity as a function of the time, only given for a short radiation time. The SA is given for the calculation with the loop and SZ effect, with only the SZ effect and with the SZ effect and the loop properties. The cut-off radiolysis fit was used.

A constant SA is reached when extraction is done after each round, because $f_{\text{radiolysis}} = 0$ for short irradiation time (approximately 4 minutes). Which results in a carrier-free batch of ^{177}Lu. The ^{177}Lu collected in the 'bulk' (on the column) will decay, however the corresponding mass does not have to be taken into account, because separation of ^{177}Hf is possible. This results in a constant specific activity in the 'bulk', for which the total activity will increase over time. Since the same fitted functions for the radiolysis have been used, the same trend for 'with' and 'without' shielding is visible as was explained for the holmium experiments. Shielding should result in a higher SA, however due to the large uncertainty in the fitted functions for the radiolysis, the SA that corresponds to 'with shielding' starts to decrease first. Furthermore, in Figure 4.19, the impact of the radiolysis on the possible specific activity is visible. Once the radiolysis is not zero anymore, the possible specific activity rapidly decreases, this is shown by the green dashed-dotted line and the blue dotted line, that correspond to the SA when there is no in between extraction.

An overview of the possible specific activities when making use of the Szilard Chalmers effect is given in Table 4.4. The SA is given when using the loop properties, with the corresponding parameters of the loop. The SA is also given for using only the SZ effect.

Table 4.4: The calculated SA [GBq/mg] at t=1500 hours, when using the SZ-affect and with SZ effect in the loop. Depending on the parameters R_e, $f_{radiolysis}$, $f_{extraction}$, $f_{relabeling}$.

R_e	Shielding	$f_{radiolysis}$	$f_{extraction}$	$f_{relabeling}$	Calculated SA(t=1500h) [GBq/mg] with loop	Calculated SA(t=1500h) [GBq/mg]
67561	No shielding	shifted	0.84	0.8	0.70	1.32
67561	FlexBeFa	shifted	0.84	0.8	1.31	2.39
1	No shielding	cut_{off}	0.84	0	89.90	1.45
1	FlexBeFa	cut_{off}	0.84	0	89.90	2.76

For comparison the specifc activity without the loop and without the SZ effect is $SA_{withoutSZ} = 0.76$ GBq/mg. This means that when the shifted $fs_{radiolysis}$ function is used with the loop, an increase of SA is achieved of a factor 1.72 and without the loop a factor of 3.27. When the cut-off radiolysis function $fc_{radiolysis}$ is used an increase of SA with the loop of a factor of 123 is achieved and when only using the SZ effect the increase is a factor 3.78.

Also for lutetium, the values are an indication of what is possible when using the SZ effect in the production loop. This is because of the large impact of the radiolysis for short irradiation times and the fitted functions for the radiolysed fractions have a large uncertainty for the short irradiation time.

Currently, commercial available ^{177}Lu is produced with specific activities of 500-592 GBq/mg [80, 81]. This is higher than the SA that is produced in the loop, this is because in the calculations natural occurring lutetium was used and the neutron flux is, in general, higher for commercial production. To achieve a higher SA, enriched Lu has to be used. Enriched lutetium of 84.44% ^{176}Lu is commercially available [25]. When enriched lutetium is used and the cut-off radiolysis function, a specific activity of 2927 GBq/mg can be achieved. However, this is again only an indication, due to the uncertainty in the fitted function. Furthermore, for lutetium also side products will be produced, such as ^{177m}Lu, but this is also already a problem when ^{177}Lu is produced via the direct route [26].

Another uncertainty in the calculation is the recoiled fraction. For the calculations of lutetium the value $F = 0.174$ has been taken from the paper of Zhernosekov et al. [14]. This value gives the fraction of retained radionuclides, that was experimentally determined for HoDOTA. The experiments could not be repeated for LuDOTA since, the HOR was not operating during the time span of this thesis. There was no literature available with this data for LuDOTA. Because there was no other value available, the value from the literature for HoDOTA has been used.

A confirmation of the code was also done for lutetium, this was done by calculating the extreme values. For lutetium the abundance of ^{176}Lu was also added as an parameter. The calculated values are compared with the maximum theoretical SA [26].

Table 4.5: The maximum possible SA [GBq/mg], calculated, calculated with the loop properties, theoretical. Depending on the parameters R_e, $f_{radiolysis}$, $f_{extraction}$, $f_{relabeling}$ and the abundance of ^{176}Lu.

R_e	$f_{radiolysis}$	$f_{extraction}$	$f_{relabeling}$	Abundance	Calculated maximum SA with SZ [GBq/mg]	Calculated maximum SA in loop [GBq/mg]	Theoretical SA [GBq/mg]
1	0	1	0	1	4104.47	4104.47	4104.47
1	0	0.84	0	1	3447.75	3447.75	3447.75
1	0	1	0	0.0259	106.31	106.31	106.31
1	0	0.84	0	0.0259	89.30	89.30	89.30

The mass check was done again, this is shown in Figure 4.20. The blue line should not cross the red dotted line, because the red dotted line shows the original mass of the target material.

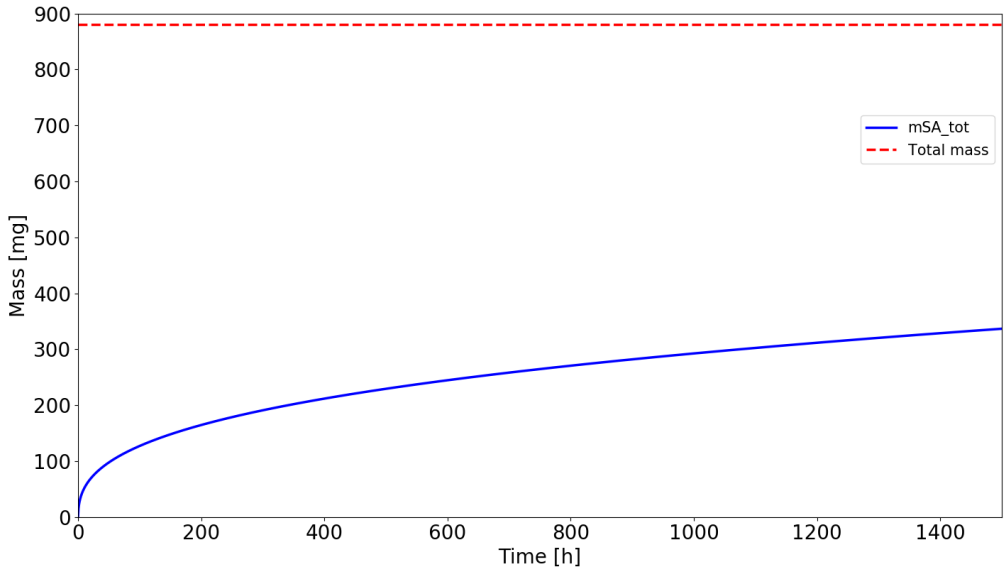

Figure 4.20: The total mass of the target material and the mass of the uncomplexed nuclides.

The code works correct, since the extreme values (carrier-free) correspond with the theoretical values. Also the mass of the uncomplexed nuclides is not higher than the mass of the target material. Furthermore, in the code an assumption that has been, is that the input material is always 0.5 L of 10 mmol HoDOTA/LuDOTA. As can be seen in Figures 4.16 and 4.20, there is a significant fraction of the mass, which is unchelated. Therefore, this assumption is only valid if after the extraction step the unlabeled DOTA is labeled again with holmium or lutetium.

In general, high specific activities can be reached when using the Szilard-Chalmers. The effect of the loop system, however, is highly dependant on the $f_{\text{radiolysis}}$ for short irradiation time. Because of the high uncertainty in the fitted functions for the fraction of radiolysis it is not certain if higher specific activities can actually be achieved when the loop is used.

5

Conclusion and Recommendations

5.1. Conclusion

It can be concluded that for lutetium, it is possible to label lutetium with DOTA, which results in a stable complex. Important for the research is that it is possible to determine the percentage of labeling with iTLC experiments. The complex is stable for longer periods of time, when kept at 40°C, which is important since this will likely be the temperature in the loop. A problem that occurred is the fast labeling of lutetium with DOTA that also happens at 40°C, which results in relabeling. The complex is affected by the gamma radiation, this can be reduced when using the FlexBeFa shielding. The fitted functions for the radiolysis effect have a large uncertainty for short irradiation time, because for short irradiation time the fitted functions gave negative values. To prevent negative values, which are not possible, the fitted functions were manipulated. For the first option the function was shifted over the y-axis. For the second option the negative values were forced to be 0. Both functions have been used in the calculations of the specific activity. DOTA itself seems to be stable under the gamma radiation. Extraction of free lutetium from LuDOTA is possible using Dowex resins. By washing with a 10^{-5} M HCl solution DOTA will remain in the solution and lutetium will remain on the resins. The lutetium can be washed off the resins with a 4 M HCl solution.

To calculate the possible specific activities with the Szilard-Chalmers effect in the loop, or only the Szilard-Chalmers effect, the experimental data for the relabeling, radiolysis and extraction were used, together with the literature value for the fraction of recoiling [14]. This results in the following maximum possible specific activities for holmium. For comparison, the specific activity without the Szilard-Chalmers effect and without the loop is $SA_{withoutSZ}$ = 0.93 GBq/mg. When using the shifted function for the radiolysis, $fs_{radiolysis}$, the calculated specific activities are $SA_{withSZloop}$ = 3.21 GBq/mg with the loop and SA_{withSZ} = 6.40 GBq/mg without the loop. This results in an increase of specific activity of a factor 3.45 with the loop and without the loop a factor of 6.88. When the cut-off radiolysis function $fc_{radiolysis}$ is used, the calculated specific activities are $SA_{withSZloop}$ = 22015 GBq/mg and SA_{withSZ} = 6.79 GBq/mg. This results in an increase of SA with the loop of a factor of 23672 and when only using the SZ effect the increase is a factor 7.30.

For lutetium the specific activity without the loop and without the SZ effect is $SA_{withoutSZ}$ = 0.76 GBq/mg. When using the shifted function for the radiolysis, the calculated specific activities are $SA_{withSZloop}$ = 1.31 GBq/mg and SA_{withSZ} = 2.39 GBq/mg. This results in an increase of specific activity of a factor 1.72 with the loop and without the loop a factor of 3.27. When the cut-off radiolysis function is used, the calculated specific activities are $SA_{withSZloop}$ = 89.9 GBq/mg, SA_{withSZ} = 2.76 GBq/mg. This is an increase of SA with the loop of a factor of 123 and when only using the SZ effect the increase is a factor 3.78.

This concludes that using the Szilard-Chalmers effect in the production of radionuclides that are produced via (n,γ) reactions, increases the specific activity. It depends on the radiolysis for short irradiation times, whether it is possible to increase the specific activity even further by using a loop system. Based on the data that was available in this thesis it was not possible to determine the radiolysis for the short irradiation time. To be able to determine if the loop system is beneficial, the effect of the gamma radiation, from the reactor core, on the stability of the complex has to be precisely determined for the first few minutes of irradiation.

5.2. Recommendations

It is important to precisely determine the effect of the gamma radiation, from the reactor core, on the stability of the complex, for the first minutes of irradiation. It is also important to investigate how the effect of radiolysis can be minimized, by investigating more gamma shielding options. A gamma shielding option could be using ascorbic acid in the loop [82], however, then also the safety regulations have to be checked.

Furthermore neutron activation experiments for LuDOTA have to be done, to determine the recoiling fraction, due to the Szilard-Chalmers effect. This parameter has for now been taken from the literature about HoDOTA, since this was the only available data. The procedure to determine the activated and recoiled fractions are described in the paper by Zhernosekov et al. [14].

The effect of the gamma radiation on the structure of DOTA should be investigated when DOTA is irradiated close to the reactor core. To have a better resolution for DOTA than the current NMR experiments, the NMR experiment should be done with samples that do not contain the buffer solution. This should give a better resolution, since in the current results the buffer has the highest intensity. The resolution will also be better if a higher molarity of the samples is used, or a larger volume is being irradiated, since both would increase the amount of DOTA being present in the NMR tubes.

In order to extract Lu from LuDOTA more experiments have to be done. The use of columns should be investigated, because these can be used in the loop. The length of the column and the velocity of the liquid through the column should be determined, for optimal extraction. In literature α-HIBA is also used to extract isotopes from the resins, this seems promising [14] and can be investigated to determine if a better extraction is possible. However, the benefit of using the HCl solutions is that it can be easily changed into a solution which can be used for treatment. Another option is to investigate whether liquid-liquid extraction is possible, because this could lead to an even more continuous process.

Lastly, it is also interesting to investigate the use of other radionuclides for the loop, such as ^{186}Re, ^{188}Re and ^{165}Dy. The investigation could first be done computationally to give an insight in the factor of increase of the specific activity.

References

[1] World Nuclear Association. Radioisotopes in industry. https://www.world-nuclear.org/information-library/non-power-nuclear-applications/radioisotopes-research/radioisotopes-in-industry.aspx. Accessed: 2021-04-13.

[2] World Nuclear Association. Radioisotopes in medicine. https://www.world-nuclear.org/information-library/non-power-nuclear-applications/radioisotopes-research/radioisotopes-in-medicine.aspx. Accessed: 2021-04-13.

[3] Michael Laing. A revised periodic table: with the lanthanides repositioned. *Foundations of Chemistry*, 7(3):203, 2005.

[4] Michiel Van de Voorde, Karen Van Hecke, Thomas Cardinaels, and Koen Binnemans. Radiochemical processing of nuclear-reactor-produced radiolanthanides for medical applications. *Coordination Chemistry Reviews*, 382:103–125, 2019.

[5] Zuzana Dvoráková. *Production and chemical processing of Lu-177 for nuclear medicine at the Munich research reactor FRM-II*. PhD thesis, Technische Universität München, 2007.

[6] D Ma, AR Ketring, GJ Ehrhardt, and W Jia. Production of radiolanthanides and radiotherapy research at murr. *Journal of radioanalytical and nuclear chemistry*, 206(1):119–126, 1996.

[7] Frank Rösch. Radiolanthanides in endoradiotherapy: an overview. *Radiochimica Acta*, 95(6):303–311, 2007.

[8] Shuang Liu and D Scott Edwards. Bifunctional chelators for therapeutic lanthanide radiopharmaceuticals. *Bioconjugate chemistry*, 12(1):7–34, 2001.

[9] Zeynep Talip, Chiara Favaretto, Susanne Geistlich, and Nicholas P van der Meulen. A step-by-step guide for the novel radiometal production for medical applications: Case studies with 68ga, 44sc, 177lu and 161tb. *Molecules*, 25(4):966, 2020.

[10] Leo Szilard and TA Chalmers. Chemical separation of the radioactive element from its bombarded isotope in the fermi effect. *Nature*, 134(3386):462–462, 1934.

[11] Zsolt Baranyai, Gyula Tircsó, and Frank Rösch. The use of the macrocyclic chelator dota in radiochemical separations. *European Journal of Inorganic Chemistry*, 2020(1):36–56, 2020.

[12] Bhupendra S Tomar, Olav M Steinebach, BE Terpstra, P Bode, and H Th Wolterbeek. Studies on production of high specific activity 99mo and 90y by szilard chalmers reaction. *Radiochimica Acta*, 98(8):499–506, 2010.

[13] Jan Willem J van Dorp, Dravin S Mahes, Peter Bode, Hubert T Wolterbeek, Antonia G Denkova, and Pablo Serra-Crespo. Towards the production of carrier-free 99mo by neutron activation of 98mo in molybdenum hexacarbonyl–szilard-chalmers enrichment. *Applied Radiation and Isotopes*, 140:138–145, 2018.

[14] KP Zhernosekov, DV Filosofov, and Frank Rösch. The szilard–chalmers effect in macrocyclic ligands to increase the specific activity of reactor-produced radiolanthanides: Experiments and explanations. *Radiochimica Acta*, 100(8-9):669–674, 2012.

[15] Leila Safavi-Tehrani. *Production of High Specific Activity Radioisotopes via the Szilard-Chalmers Method, Using the UC-Irvine TRIGA® Reactor*. PhD thesis, UC Irvine, 2016.

[16] S Zeisler and K Weber. Szilard-chalmers effect in holmium complexes. *Journal of radioanalytical and nuclear chemistry*, 227(1-2):105–109, 1998.

[17] Zhiyong Zhang, Xiangyun Wang, Yonghui Wu, Yuanfang Liu, Wuqin Zheng, and Ke Wang. Preparation of 186re and 188re with high specific activity by the szilard–chalmers effect. *Journal of Labelled Compounds and Radiopharmaceuticals: The Official Journal of the International Isotope Society*, 43(1):55–64, 2000.

[18] Syed M Qaim and Ingo Spahn. Development of novel radionuclides for medical applications. *Journal of Labelled Compounds and Radiopharmaceuticals*, 61(3):126–140, 2018.

[19] Raphael Lengacher and Roger Alberto. Bioorganometallics: 99mtc cytectrenes, syntheses and applications in nuclear medicine. *Coordination Chemistry Reviews*, 437:213869, 2021.

[20] Alan H Maurer. Combined imaging modalities: Pet/ct and spect/ct. *Health physics*, 95(5):571–576, 2008.

[21] Misara Hamoudeh, Muhammad Anas Kamleh, Roudayna Diab, and Hatem Fessi. Radionuclides delivery systems for nuclear imaging and radiotherapy of cancer. *Advanced drug delivery reviews*, 60(12):1329–1346, 2008.

[22] Sophie Poty, Lynn C Francesconi, Michael R McDevitt, Michael J Morris, and Jason S Lewis. α-emitters for radiotherapy: From basic radiochemistry to clinical studies—part 1. *Journal of Nuclear Medicine*, 59(6):878–884, 2018.

[23] Nienke JM Klaassen, Mark J Arntz, Alexandra Gil Arranja, Joey Roosen, and J Frank W Nijsen. The various therapeutic applications of the medical isotope holmium-166: a narrative review. *EJNMMI radiopharmacy and chemistry*, 4(1):19, 2019.

[24] Jean-Pierre Pouget, Catherine Lozza, Emmanuel Deshayes, Vincent Boudousq, and Isabelle Navarro-Teulon. Introduction to radiobiology of targeted radionuclide therapy. *Frontiers in medicine*, 2:12, 2015.

[25] R Bhardwaj. *Radionuclide generator based production of therapeutic lutetium-177*. PhD thesis, Delft University of Technology, 2019.

[26] Ashutosh Dash, Maroor Raghavan Ambikalmajan Pillai, and Furn F Knapp. Production of 177 lu for targeted radionuclide therapy: available options. *Nuclear medicine and molecular imaging*, 49(2):85–107, 2015.

[27] Vladimir Tolmachev, Jörgen Carlsson, and Hans Lundqvist. A limiting factor for the progress of radionuclide-based cancer diagnostics and therapy availability of suitable radionuclides. *Acta Oncologica*, 43(3):264–275, 2004.

[28] JJM De Goeij and ML Bonardi. How do we define the concepts specific activity, radioactive concentration, carrier, carrier-free and no-carrier-added? *Journal of radioanalytical and nuclear chemistry*, 263(1):13–18, 2005.

[29] Rachel A Morneau. Development of 166ho skin patch to treat skin diseases with 1 mw triga reactor, 2014.

[30] IAEA. Live chart of nuclides. `https://www-nds.iaea.org/relnsd/vcharthtml/VChartHTML.html`. Accessed: 2020-10-28.

[31] Alexander W Chao and Weiren Chou. *Reviews Of Accelerator Science And Technology-Volume 2: Medical Applications Of Accelerators*. World Scientific, 2009.

[32] M Haji-Saeid and M.R.A Pillai. *Cyclotron produced radionuclides-physical characteristics and production methods*. Internat. Atomic Energy Agency, 2009.

[33] Attila Vértes, Sándor Nagy, Zoltán Klencsár, Rezso György Lovas, and Frank Rösch. *Handbook of Nuclear Chemistry: Vol. 1: Basics of Nuclear Science; Vol. 2: Elements and Isotopes: Formation, Transformation, Distribution; Vol. 3: Chemical Applications of Nuclear Reactions and Radiation; Vol. 4: Radiochemistry and Radiopharmaceutical Chemistry in Life Sciences; Vol. 5: Instrumentation, Separation Techniques, Environmental Issues; Vol. 6: Nuclear Energy Production and Safety Issues*. Springer Science & Business Media, 2010.

[34] Sharmila Banerjee, MRA Pillai, and FF Knapp. Lutetium-177 therapeutic radiopharmaceuticals: linking chemistry, radiochemistry, and practical applications. *Chemical reviews*, 115(8):2934–2974, 2015.

[35] Christoph Barkhausen. *Production of non carrier added (nca) 177 Lu for radiopharmaceutical applications*. PhD thesis, Technische Universität München, 2011.

[36] Menno Blaauw, D Ridikas, S Baytelesov, PS Bedregal Salas, Y Chakrova, Cho Eun-Ha, R Dahalan, AH Fortunato, R Jacimovic, A Kling, et al. Estimation of 99 mo production rates from natural molybdenum in research reactors. *Journal of radioanalytical and nuclear chemistry*, 311(1):409–418, 2017.

[37] Leila Safavi-Tehrani, George E Miller, and Mikael Nilsson. Production of high specific activity radiolanthanides for medical purposes using the uc irvine triga reactor. *Journal of Radioanalytical and Nuclear Chemistry*, 303(2):1099–1103, 2015.

[38] Gregory Choppin, Jan-Olov Liljenzin, and Jan Rydberg. *Radiochemistry and nuclear chemistry*. Butterworth-Heinemann, 2002.

[39] Gerhart Friedlander, Joseph W Kennedy, Edward S Macias, and Julian M Miller. *Nuclear and radiochemistry*. John Wiley & Sons, 1981.

[40] SK Morcos. Extracellular gadolinium contrast agents: differences in stability. *European journal of radiology*, 66(2):175–179, 2008.

[41] Xiangyang Liang and Peter J Sadler. Cyclam complexes and their applications in medicine. *Chemical Society Reviews*, 33(4):246–266, 2004.

[42] PL Edelin De La Praudiere and LAK Staveley. Thermodynamics of the formation of the 1: 1 complexes of nitrilotriacetic acid and rare earth ions. *Journal of Inorganic and Nuclear Chemistry*, 26(10):1713–1719, 1964.

[43] Dojindo Molecular Technologies inc. Metal chelates. `https://www.dojindo.eu.com/images/Product%20Photo/Chelate_Table_of_Stability_Constants.pdf`. Accessed: 2020-09-23.

[44] Michaela Koudelková, Hana Vinšová, and Věra Jedináková-Křižová. Isotachophoretic determination of stability constants of ho and y complexes with diethylenetriaminepentaacetic acid and 1, 4, 7, 10-tetraazadodecane-n, n, n , n-tetraacetic acid. *Journal of Chromatography A*, 990(1-2):311–316, 2003.

[45] E Moutiez, P Prognon, G Mahuzier, P Bourrinet, S Zehaf, and A Dencausse. Time-resolved luminescence as a novel detection mode for the simultaneous high-performance liquid chromatographic determination of gadolinium–dota and gd3+. *Analyst*, 122(11):1347–1352, 1997.

[46] August Winkelman. Neutron spectrum dldr tube. 2021.

[47] Frans De Corte. The updated naa nuclear data library derived from the y2k k0-database. *Journal of radioanalytical and nuclear chemistry*, 257(3):493–499, 2003.

[48] R Van Grieken and M De Bruin. Nomenclature for radioanalytical chemistry (iupac recommendations 1994). *Pure and Applied Chemistry*, 66(12):2520, 1994.

[49] Satoshi Watanabe, Kazuyuki Hashimoto, Shigeki Watanabe, Yasuhiko Iida, Hirofumi Hanaoka, Keigo Endo, and Noriko S Ishioka. Production of highly purified no-carrier-added 177 lu for radioimmunotherapy. *Journal of Radioanalytical and Nuclear Chemistry*, 303(1):935–940, 2015.

[50] Muhammad U Akbar, Tanveer H Bokhari, Muhammad R Ahmad, Khalid M Zia, Samina Roohi, Nimra Ayub, and Muhammad Sohaib. Radiosynthesis, radiochemical, and biological characterization of 177lu-labeled diethylenetriamine penta-acetic acid. *Journal of cellular biochemistry*, 120(9):14510–14517, 2019.

[51] Jonathan Clayden, Nick Greeves, and Stuart Warren. Organic chemistry, 2012.

[52] Antonia Denkova. Flexbefa. 2019.

[53] A Dean Sherry, Peter Caravan, and Robert E Lenkinski. Primer on gadolinium chemistry. *Journal of Magnetic Resonance Imaging: An Official Journal of the International Society for Magnetic Resonance in Medicine*, 30(6):1240–1248, 2009.

[54] Sigma Aldrich. Ion exchange resins: Classification and properties. https://www.sigmaaldrich.com/content/dam/sigma-aldrich/docs/Aldrich/Brochure/al_pp_ionx.pdf. Accessed: 2021-03-25.

[55] Jack Schubert. The use of ion exchangers of the determination of physical-chemical properties of substances, particularly radiotracers, in solution. i. theoretical. *The Journal of Physical Chemistry*, 52(2):340–350, 1948.

[56] J Kenneth Shultis and Richard E Faw. *Fundamentals of Nuclear Science and Engineering Third Edition*. CRC press, 2016.

[57] *Quality Control of Radiopharmaceuticals*, pages 151–174. Springer New York, New York, NY, 2004.

[58] Archana A Bele and Anubha Khale. An overview on thin layer chromatography. *International Journal of Pharmaceutical Sciences and Research*, 2(2):256, 2011.

[59] C Decristoforo, I Zolle, F Rakiás, J Imre, Gy Jánoki, and SR Hesslewood. Quality control methods of 99m tc pharmaceuticals. In *Technetium-99m Pharmaceuticals*, pages 123–150. Springer, 2007.

[60] Christopher Burgess. The basis for good spectrophotometric uv–visible measurements. In *UV-Visible Spectrophotometry of Water and Wastewater*, pages 1–35. Elsevier, 2017.

[61] Stephen Mezyk, Kristian Larsson, Rocklan McDowell, and Leigh Martin. Elucidation of the kinetics of advanced separation systems. Technical report, Stephen Mezyk, 2020.

[62] Miguel Angel Hernández-García, Hilario López-González, Alberto Rojas-Hernández, et al. Hydrolysis of trivalent holmium in aqueous solutions of 2 m ionic strength by spectrophotometric and potentiometric methods. *Advances in Materials Physics and Chemistry*, 5(05):161, 2015.

[63] Jens-Uwe Kunstler, Gesine Seidel, and Hans-Jurgen Pietzsch. Efficient preparation of 99mtc (iii)'4+ 1'mixed-ligand complexes for peptide labeling with high specific activity. *Applied Radiation and Isotopes*, 68(9):1728–1733, 2010.

[64] Hassan Yousefnia, Edalat Radfar, Amir Jalilian, Ali Bahrami-Samani, Simindokht Shirvani-Arani, Azim Arbabi, and Mohammad Ghannadi-Maragheh. Development of 177lu-dota-anti-cd20 for radioimmunotherapy. *Journal of Radioanalytical and Nuclear Chemistry*, 287(1):199–209, 2011.

[65] J Charlotte Fowler, Chandra K Solanki, Robert W Barber, James R Ballinger, and A Michael Peters. Dual-isotope lymphoscintigraphy using albumin nanocolloid differentially labeled with 111in and 99mtc. *Acta Oncologica*, 46(1):105–110, 2007.

[66] Astrid Van der Meer. Tlc for labeling efficiency 225ac-dota-polymers, 111in-dtpa, 213bi-dtpa-pluronics.

[67] A Gandhi, Aman Sharma, Rebecca Pachuau, B Lalremruata, Mayur Mehta, Prashant N Patil, SV Suryanarayana, LS Danu, BK Nayak, and A Kumar. Neutron radiative capture cross section for sodium with covariance analysis. *The European Physical Journal A*, 57(1):1–12, 2021.

[68] T Wright, S Bennett, S Heinitz, U Köster, R Mills, T Soldner, Peter Steier, Anton Wallner, and T Wieninger. Measurement of the 13 c (n, \ gamma γ) thermal cross section via neutron irradiation and ams. *The European Physical Journal A*, 55(11):1–7, 2019.

[69] Ė Tóth and E Brücher. Stability constants of the lanthanide (iii)-1, 4, 7, 10-tetraazacyclododecane-n, n, n , n-tetraacetate complexes. *Inorganica chimica acta*, 221(1-2):165–167, 1994.

[70] Chemistry Steps. Nmr chemical shift values table. https://www.chemistrysteps.com/nmr-chemical-shift-values-table/. Accessed: 2021-04-07.

[71] BingYang Chu, Lan Zhang, Ying Qu, XiaoXin Chen, JinRong Peng, YiXing Huang, and ZhiYong Qian. Synthesis, characterization and drug loading property of monomethoxy-poly (ethylene glycol)-poly (ε-caprolactone)-poly (d, l-lactide)(mpeg-pcla) copolymers. *Scientific reports*, 6(1):1–15, 2016.

[72] M Emília Azenha, Hugh D Burrows, Sofia M Fonseca, M Luísa Ramos, Jose Rovisco, J Seixas de Melo, Abilio JFN Sobral, and Ksenija Kogej. Luminescence from cerium (iii) acetate complexes in aqueous solution: considerations on the nature of carboxylate binding to trivalent lanthanides. *New Journal of Chemistry*, 32(9):1531–1535, 2008.

[73] Andoni Zuriarrain, Juan Zuriarrain, Ana Isabel Puertas, María Teresa Dueñas, and Iñaki Berregi. Quantitative determination of lactic and acetic acids in cider by 1h nmr spectrometry. *Food Control*, 52:49–53, 2015.

[74] Yohan Jeong and Kun Na. Synthesis of a gadolinium based-macrocyclic mri contrast agent for effective cancer diagnosis. *Biomaterials research*, 22(1):1–8, 2018.

[75] Matthias Ceulemans, Koen Nuyts, Wim M De Borggraeve, and Tatjana N Parac-Vogt. Gadolinium (iii)-dota complex functionalized with bodipy as a potential bimodal contrast agent for mri and optical imaging. *Inorganics*, 3(4):516–533, 2015.

[76] Odd B Michelsen and Morton Smutz. Separation of yttrium, holmium, and erbium with di-(2-ethylhexyl) phosphoric acid in chloride and nitrate systems. *Journal of Inorganic and Nuclear Chemistry*, 33(1):265–278, 1971.

[77] Tapas Das, Sudipta Chakraborty, Haladhar D Sarma, Meera Venkatesh, and Sharmila Banerjee. Preparation of 166ho-oxine-lipiodol and its preliminary bioevaluation for the potential application in therapy of liver cancer. *Nuclear Medicine Communications*, 30(5):362–367, 2009.

[78] Nafise Salek, Sara Vosoughi, Ali Bahrami Samani, Simindokht Shirvani Arani, and Mohammad Ghannadi Maragheh. Radiolabeled tpp with 166 dy/166 ho in vivo generator as a novel therapeutic agent. *Journal of Radioanalytical and Nuclear Chemistry*, 326(1):813–821, 2020.

[79] Andrey G Kazakov, Sergey S Belyshev, Taisya Yu Ekatova, Vadim V Khankin, Alexander A Kuznetsov, and Ramiz A Aliev. Production of 177 lu by hafnium irradiation using 55-mev bremsstrahlung photons. *Journal of Radioanalytical and Nuclear Chemistry*, 317(3):1469–1476, 2018.

[80] Priya Bhusari, Rakhee Vatsa, Gurpreet Singh, Madan Parmar, Amanjit Bal, Devinder K Dhawan, Bhagwant R Mittal, and Jaya Shukla. Development of lu-177-trastuzumab for radioimmunotherapy of her2 expressing breast cancer and its feasibility assessment in breast cancer patients. *International journal of cancer*, 140(4):938–947, 2017.

[81] IDB Holland. Lumark lu-177 chloride. `https://www.idb-holland.com/our-products/lutetium-177-lumark/`. Accessed: 2021-04-20.

[82] Michele Iori, Pier C Capponi, Sara Rubagotti, Luca Rosario Esposizione, Johanna Seemann, Riccardo Pitzschler, Thorsten Dreger, Debora Formisano, Elisa Grassi, Federica Fioroni, et al. Labelling of y- and lu-dota-bioconjugates for targeted radionuclide therapy: a comparison among manual, semiautomated, and fully automated synthesis. *Contrast media & molecular imaging*, 2017, 2017.

A

Appendix

In Figure A.1 the fitted function of the stability as a function of the time in the DLDR tube is given. In Figure A.2 the fitted function of the stability as a function of the time in the DLDR tube with the FlexBeFa shielding is given. The data points correspond to the data points, that were measured using the ^{60}Co source.

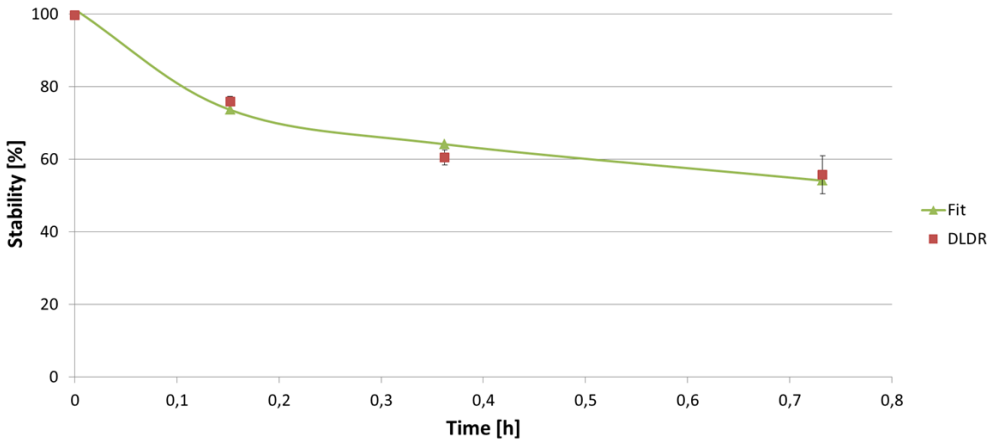

Figure A.1: The fitted function for the stability as a function of the time in the DLDR tube.

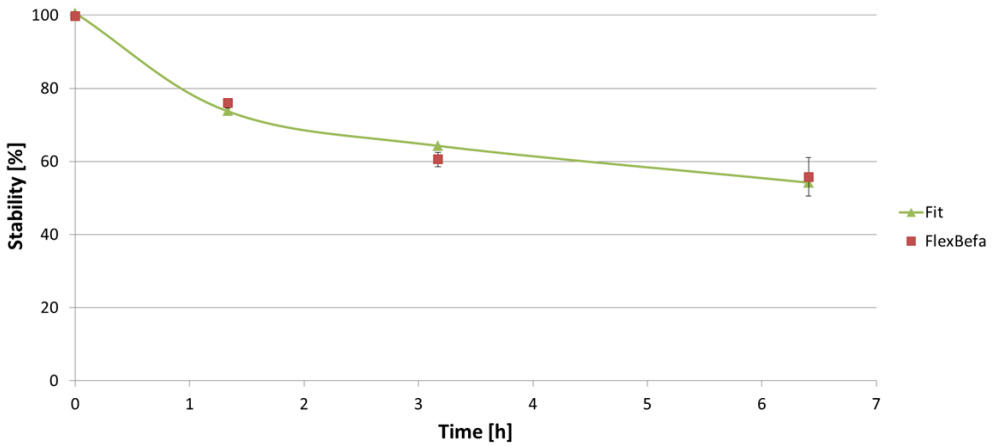

Figure A.2: The fitted function for the stability as a function of the time in the DLDR tube with shielding.

In Figure A.3 the specific activity as a function of the time for holmium is given, for the irradiation time of t=240 hours. For this calculation the cut-off fitted function for the radiolysis was used. In Figure A.4 the specific activity as a function of time is given, when the mass of the decay product is taken into account. This results in a decrease of the specific activity, due to the decay of ^{166}Ho to ^{166}Er. The lines for 'Without loop and SZ effect', 'With SZ effect with shielding' and 'With SZ effect without shielding' appear to be zero, however, this is only because of the scale of the y-axis.

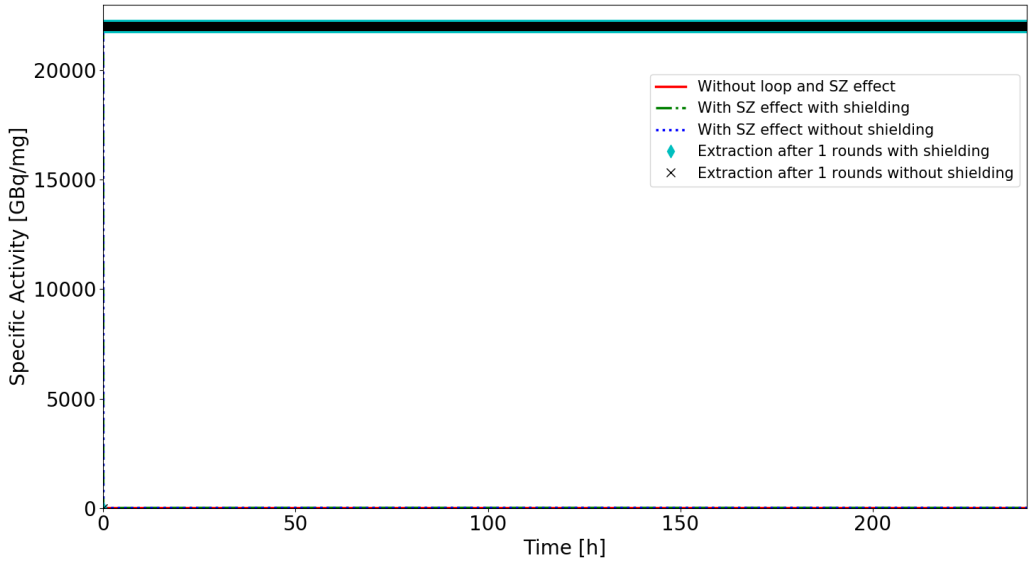

Figure A.3: The specific activity as a function of the time for holmium. Calculated with the cut-off fitted function for the fraction of radiolysis.

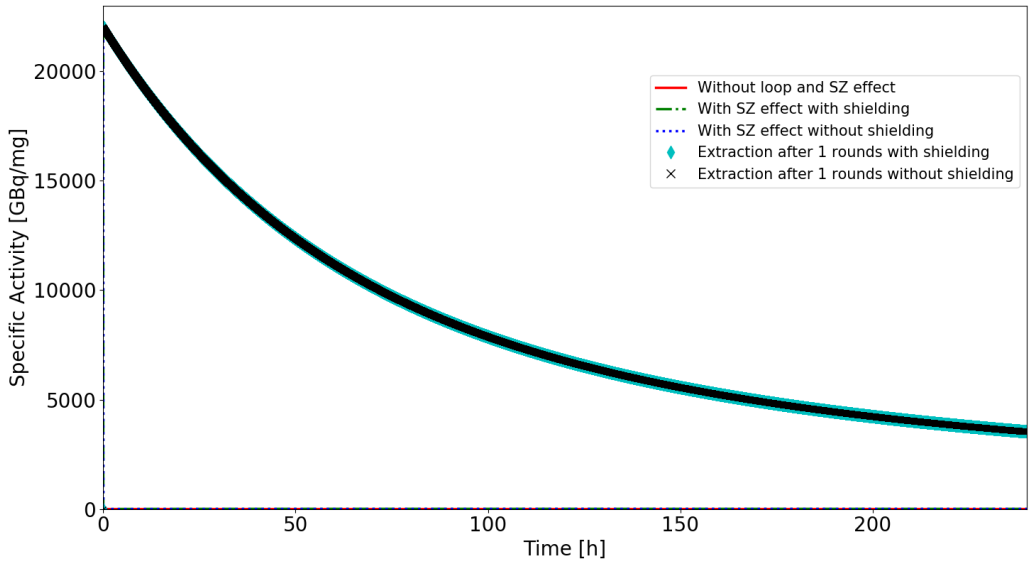

Figure A.4: The specific activity as a function of the time for holmium, when taking into account the mass of the decay product. Calculated with the cut-off fitted function for the fraction of radiolysis.

In Figure A.5 for lutetium the specific activity as a function of the time is given for the irradiation time of t=1500 hours. For this calculation the cut-off fitted function for the radiolysis was used. In Figure A.6 the specific activity as a function of time is given, when the mass of the decay product is taken into account. This results in a decrease of the specific activity, due to the decay of ^{177}Lu to ^{177}Hf.

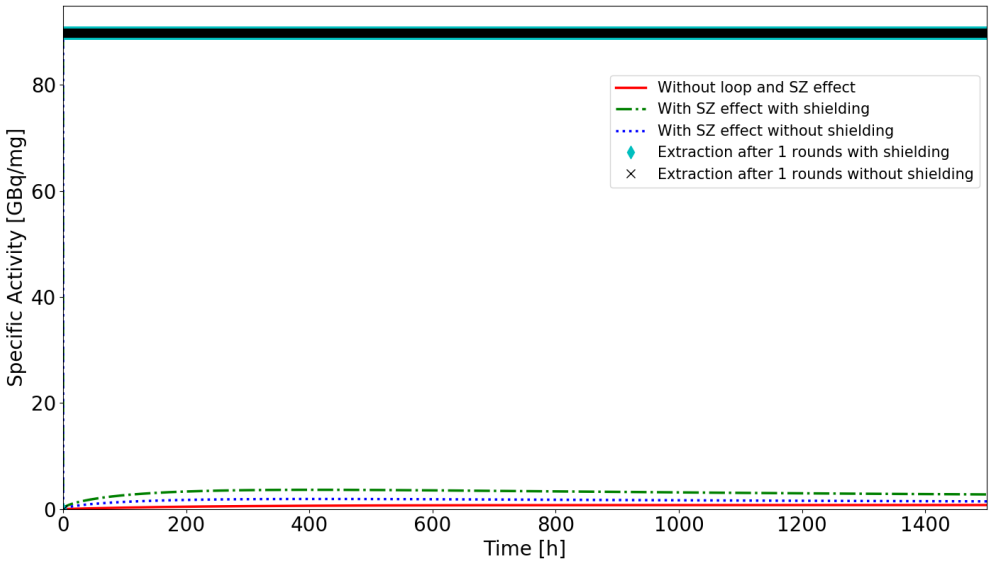

Figure A.5: The specific activity as a function of the time for lutetium. Calculated with the cut-off fitted function for the fraction of radiolysis.

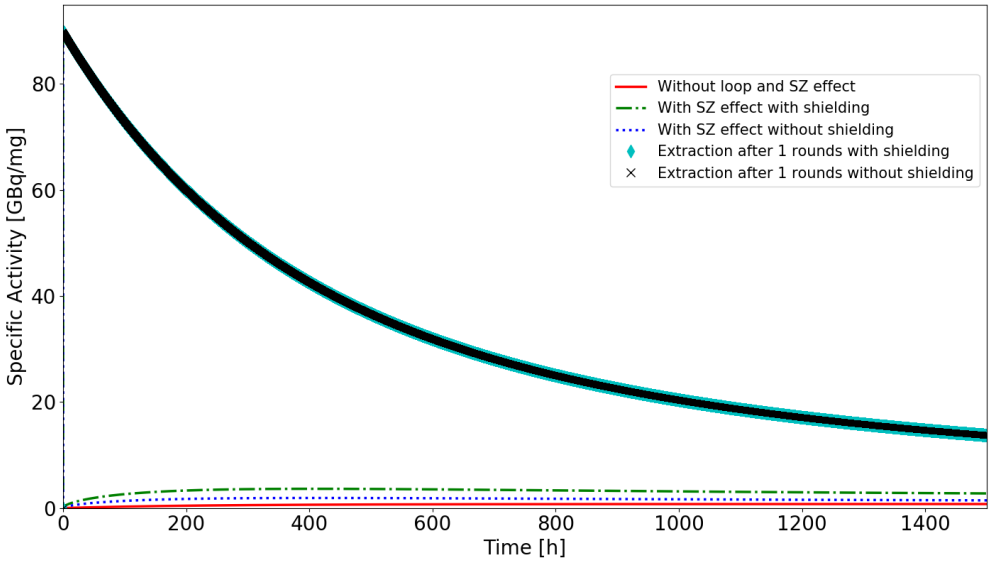

Figure A.6: The specific activity as a function of the time for lutetium. Calculated with the cut-off fitted function for the fraction of radiolysis.

B

Appendix

The code to calculate the specific activity is given below. The functions were placed in a different Python file and imported into the main file. This results in three separate Python files: main.py, functions.py and plotfunctions.py.

The main file main.py:

```
import numpy as np
import plotfunction as pf
import functions as f

#Input parameters
V = 0.5 #In liters
t_irr =1500 #In hours 1500 for Lu, 240 for Ho
R_e = 1 #Number of rounds before separation

# Constants
NA = 6.022*10**23 #Avogadros number particles/mol
phi = 4.25*10**12  #Neutron flux from HOR in seconds
phi_e = 0.156*10**11 #Epithermic neutron flux at 1 eV [neutrons/cm2s]

# Constants Radionuclide
matType = f.Lutetium()

# Experimental parameters
molarity = 0.01 #Amount of mol/L Lu input
dx = 0.15*4 #Length of the irradiated part of the loop in meters
v = 0.025 #Velocity minimum in m/s
t_Round = int(dx/v) #Time of one round in seconds
t_irr_sec = t_irr*3600
Rounds_max = int(t_irr_sec/t_Round) #Number of rounds in the irradation time
t = np.linspace(0,t_irr_sec,Rounds_max)
t_max = R_e*t_Round #Time before separation

# Choose one of the f_relabeling below, depending on the extraction time
f_relabeling = 1 #For extraction after 1*t_Round
#f_relabeling = 0.2 #For extraction after >100*t_Round

# Constans from Experiments
R = 0.132 #Retention factor from Zhernosekov
f_extraction = 1-0.16 #Chemically separable nuclides
```

```
# Calculations Loop
N_0, mtot = f.Nin(NA, molarity,V,matType) #number of target (input) atoms
Nsz, f_recoil = f.SZ_activation(N_0,phi,t,phi_e,matType,R,Rounds_max, t_Round)
#Szilard Chalmers effect

# Choose with or without the effects of the FlexBeFa
mSA_act, mSA, f_radiolysis = f.massfraction(t, f_recoil, mtot, f_relabeling)
#Gamma radiation effect
mSA_act_f, mSA_f, f_radiolysis_f = f.massfractionFlexBeFa(t, f_recoil, mtot,
f_relabeling) #Gamma radiation effect FlexBeFa

SA, Atot = f.Activity(matType, Nsz, mSA,f_relabeling,f_extraction, mSA_act)
#(Specific) activity due to Szilard Chalmers effect
SA_f, Atot_f = f.Activity(matType, Nsz, mSA_f,f_relabeling,f_extraction, mSA_act_f)
#(Specific) activity due to Szilard Chalmers effect with FlexBeFa

N_batch, t_batch, Nsz_batch, mSA_batch, mSA_act_batch =
f.batch(t_irr_sec,t_max,Nsz,R_e,f_relabeling, mSA, mSA_act)
#Number of batches and Nsz per batch
N_batch_f, t_batch_f, Nsz_batch_f, mSA_batch_f, mSA_act_batch_f =
f.batch(t_irr_sec,t_max,Nsz,R_e,f_relabeling,mSA_f,mSA_act_f)
#Number of batches and Nsz per batch

SA_loop, SA_bulk =
f.bulk(matType,N_batch,Nsz_batch,t_max,f_extraction,mSA_batch,mSA_act_batch)
#Calculation of the SA in the end, taking decay into account
SA_loop_f, SA_bulk_f =
f.bulk(matType,N_batch_f,Nsz_batch_f,t_max,f_extraction,mSA_batch_f,mSA_act_batch_f)
#Calculation of the SA in the end, taking decay into account

#Calculation of SA without Szilard Chalmer or the loop
t_normal = np.linspace(0,t_irr_sec,t_irr_sec)
SA_normal = f.SAnormal(matType,N_0,phi,phi_e,t_normal,mtot)

#Plot functions
t_plot = np.linspace(0,t_irr,Rounds_max-1) #x-axis for the plots
t_plot_batch = (t_batch)/3600
t_plot_normal = t_normal/3600

fig1 = pf.myFigure(['Time␣[h]', 'Mass␣[mg]'],0,900,0,t_irr)
fig1.addLine(t_plot, (mSA[1:]+mSA_act[1:]), 'b-', 'mSA_tot')
fig1.addLine([0,t_irr],[mtot,mtot], 'r--', 'Total␣mass')

fig2 = pf.myFigure(['Time␣[h]', 'Fraction␣of␣radiolysis'],0,0.4,0,t_irr)
fig2.addLine(t/3600, f_radiolysis, 'r--', 'Radiolysis')
fig2.addLine(t/3600, f_radiolysis_f, 'b-', 'Radiolysis␣with␣shielding')

fig3 = pf.myFigure(['Time␣[h]', 'Specific␣Activity␣[GBq/mg]'],0,110,0,t_irr)
fig3.addLine(t_plot_normal, SA_normal, 'r-', 'Without␣loop␣and␣SZ␣effect')
fig3.addLine(t_plot, SA_f, 'g-.', 'With␣SZ␣effect␣with␣shielding')
fig3.addLine(t_plot, SA, 'b:', 'With␣SZ␣effect␣without␣shielding')
fig3.addLine(t_plot_batch, SA_loop_f, 'cd', 'Extraction␣after␣' + str(R_e) +
'␣rounds␣with␣shielding')
fig3.addLine(t_plot_batch, SA_loop, 'kx', 'Extraction␣after␣' + str(R_e) +
'␣rounds␣without␣shielding')
```

functions.py:

```
import numpy as np
import operator
class Material():

    def __init__(self, x, thalf, sigma_act, h, M, I0):
        self.x = x
        self.labda = np.log(2)/(thalf)
        self.sigma_act = sigma_act
        self.h = h
        self.M = M
        self.I0 = I0

def Lutetium():
    material = Material( 'Lutetium',
                         6.65*24*60*60, #In seconds from 177
                         2020*10**-24, #Cross section from 176 to 177
                         2.59/100, #abundance depends on the enrichment of 176
                         175, #Molar mass
                         1000*10**-24) #resonance integral epithermal neutrons
    return material

def Lutetiumenriched():
    material = Material( 'Lutetium enriched',
                         6.65*24*60*60, #In seconds from 177
                         2020*10**-24, #Cross section from 176 to 177
                         84.44/100, #abundance depends on the enrichment of 176
                         175, #Molar mass
                         1000*10**-24) #resonance integral epithermal neutrons
    return material

def Holmium():
    material = Material( 'Holmium',
                         26.824*60*60, #In seconds from 166
                         58*10**-24, #Cross section from 165 to 166
                         1, #abundance depends on the enrichment of 165
                         164.9, #Molar mass
                         632*10**-24) #resonance integral epithermal neutrons
    return material

def Nin(NA, molarity, V, matType):
    N = NA*molarity*V*matType.h
    mtot = V*molarity*matType.M*10**3 #in mg
    return N, mtot

def SZ_activation(N_0, phi, t, phi_e, matType, R, Rounds_max, t_Round):
    Nsz = np.zeros((Rounds_max))
    f_recoil = np.zeros((Rounds_max))
    for i in range(Rounds_max):
        Nsz[i] = (phi*matType.sigma_act+phi_e*matType.I0)*N_0*(1-R)*
        (1-np.exp(-matType.labda*t[i]))/matType.labda
        #Nsz in each round
        f_recoil[i] = Nsz[i]/N_0

    return Nsz, f_recoil
```

```
def massfraction(t, f_recoil, mtot, f_relabeling):
    #Shifted radiolysis function
    #f_radiolysis = (100-(-3.246*((t)/3600)**0.3397+100.0))/100
    #Cut-off radiolysis function
    f_radiolysis = (100-(-3.246*((t)/3600)**0.3397+101.3))/100
    condition = (f_radiolysis<0)
    f_radiolysis[condition] = 0

    mSA_act = (f_recoil)*mtot
    mSA = (f_radiolysis*f_relabeling)*mtot

    return mSA_act, mSA, f_radiolysis

def massfractionFlexBeFa(t, f_recoil, mtot, f_relabeling):
    #Shifted radiolysis function
    f_radiolysis = (100-(-1.584*((t)/3600)**0.3474+100.0))/100
    #Cut-off radiolysis function
    f_radiolysis = (100-(-1.584*((t)/3600)**0.3474+100.6))/100
    condition = (f_radiolysis<0)
    f_radiolysis[condition] = 0

    mSA_act = (f_recoil)*mtot
    mSA = (f_radiolysis*0.2)*mtot

    return mSA_act, mSA ,f_radiolysis


def Activity(matType,Nsz,mSA,f_relabeling,f_extraction, mSA_act):
    Atot = matType.labda*Nsz[1:]*10**-9
    SA = Atot/(mSA[1:]+mSA_act[1:])*f_relabeling*f_extraction

    return SA, Atot

def batch(t_irr_sec,t_max,Nsz,R_e,f_relabeling, mSA, mSA_act):
    N_batch = int(round(t_irr_sec/t_max))
    t_batch = np.linspace(0,N_batch-1,N_batch)*t_max

    Nsz_batch = Nsz[R_e]*f_relabeling
    mSA_batch = mSA[R_e]
    mSA_act_batch = mSA_act[R_e]

    return N_batch, t_batch, Nsz_batch, mSA_batch, mSA_act_batch

def bulk(matType,N_batch,Nsz_batch,t_max,f_extraction,mSA_batch,mSA_act_batch):
    Nsz_bulk = np.zeros((N_batch))
    mSA_bulk = np.zeros((N_batch))
    mSA_act_bulk = np.zeros((N_batch))
    SA_bulk = np.zeros((N_batch))

    for i in range(N_batch-1):
        Nsz_bulk[i+1] = Nsz_batch+Nsz_bulk[i]*(np.exp(-matType.labda*t_max))
        mSA_bulk[i+1] = mSA_batch+mSA_bulk[i]
        mSA_act_bulk[i+1] = mSA_act_batch+mSA_act_bulk[i]*np.exp(-matType.labda*t_max)
        SA_bulk[i+1] = matType.labda*Nsz_bulk[i+1]/(mSA_bulk[i+1]+mSA_act_bulk[i+1])*10**-9

    SA_loop = SA_bulk*f_extraction
```

```
    return SA_loop, SA_bulk

def SAnormal(matType,N_0,phi,phi_e,t_normal,mtot):
    SA_normal = 10**-9*(N_0*(phi*matType.sigma_act+phi_e*matType.I0)
    *(1-np.exp(-matType.labda*t_normal)))/(mtot)

    return SA_normal
```

plotfunctions.py

```
import matplotlib.pyplot as plt
from matplotlib import cm
global plt

class myFigure():
    def __init__( self, label, bottom, top, left, right ):
        self.plt, self.ax = plt.subplots(1)
        #self.plot = plt.figure()
        self.ax.set_ylim(bottom,top)
        self.ax.set_xlim(left,right)
        self.ax.tick_params(axis='both', which='major', labelsize=20)
        self.ax.set_xlabel(str(label[0]), fontsize=20)
        self.ax.set_ylabel(str(label[1]), fontsize=20)
        plt.ion()
        self.plt.show()
        self.legend = False

    def addLine( self, x, y, font, legend):

        if font[0]=='c':
            markersize = 9
        else:
            markersize = 7
        self.ax.plot(x,y, font, label=legend, markersize=markersize, linewidth=2.5)
        self.ax.legend(fontsize=15, loc=7, bbox_to_anchor=(1, 0.75))
```